Searches for Higgs pair production using the CMS detector

Souvik Das on behalf of the **CMS Collaboration**

Higgs Pair Production at Colliders
Mainz Institute for Theoretical Physics
Johannes Gutenberg University
27 April 2015

Outline

How well will CMS measure the SM di-Higgs production cross section?

Outline

How well will CMS measure the SM di-Higgs production cross section?

- Results of **future studies** to measure SM non-resonant di-Higgs production
  - $HH \rightarrow (\gamma\gamma)(b\bar{b})$ shown
  - $HH \rightarrow (WW)(bb)$ shown
  - $HH \rightarrow (\tau\tau)(bb)$ under approval

Outline

How well will CMS measure the SM di-Higgs production cross section?

- Results of **future studies** to measure SM non-resonant di-Higgs production
  - $HH \rightarrow (\gamma\gamma)(b\bar{b})$ shown
  - $HH \rightarrow (WW)(bb)$ shown
  - $HH \rightarrow (\tau\tau)(bb)$ under approval

- With Run 1 data we placed limits on pair-production due to BSM physics
  - **Resonant HH**. 4 b-jet final state. $X \rightarrow HH \rightarrow (b\bar{b})(b\bar{b})$
  - **Resonant HH**. 2 photons and 2 b-jets final state. $X \rightarrow HH \rightarrow (\gamma\gamma)(b\bar{b})$
  - **Non-resonant HH**. multi-leptons and photons final state: $X \rightarrow HH \rightarrow (ll)(ll/\gamma)$

Resonant is easier since we can exploit m_X. Experience gained with beating pileup, b-tagging, Higgs pairing.

Non-resonant HH production

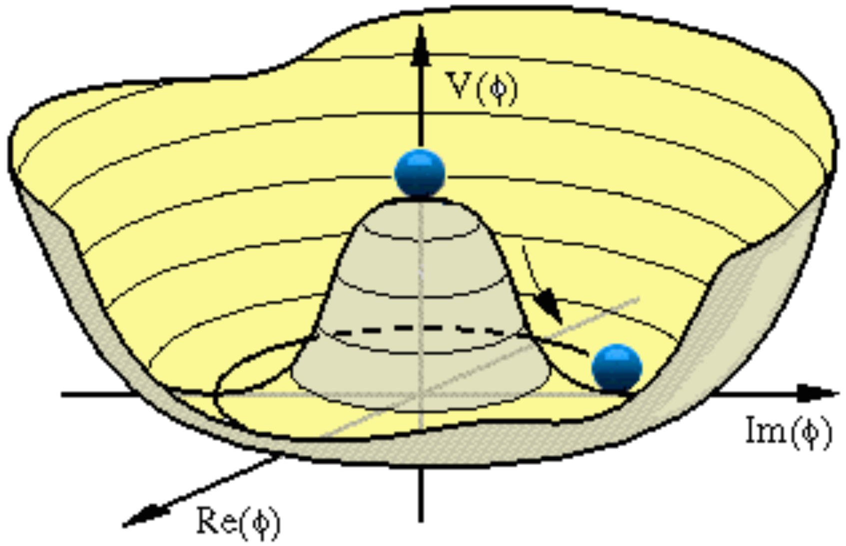

$$V(\phi) = -m^2|\phi|^2 + \lambda|\phi|^4$$

Expanding around the VEV after EWSB,: $\phi = \begin{pmatrix} 0 \\ \frac{v+H(x)}{\sqrt{2}} \end{pmatrix}$
we see the trilinear and quartic self-coupling of the Higgs

$$V(H) = \frac{m_H^2}{2}H^2 + \boxed{\frac{m_H^2}{2v}H^3} + \frac{m_H^2}{8v^2}H^4$$

- Quartic coupling out of reach of LHC & HL-LHC, but **trilinear coupling accessible with 3 ab^{-1}**. SM HH cross section at 14 TeV is 40.2 fb [NNLO]

- Destructive interference between diagrams:

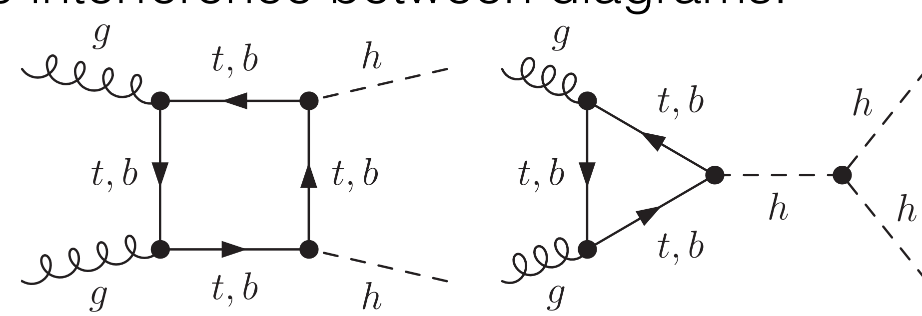

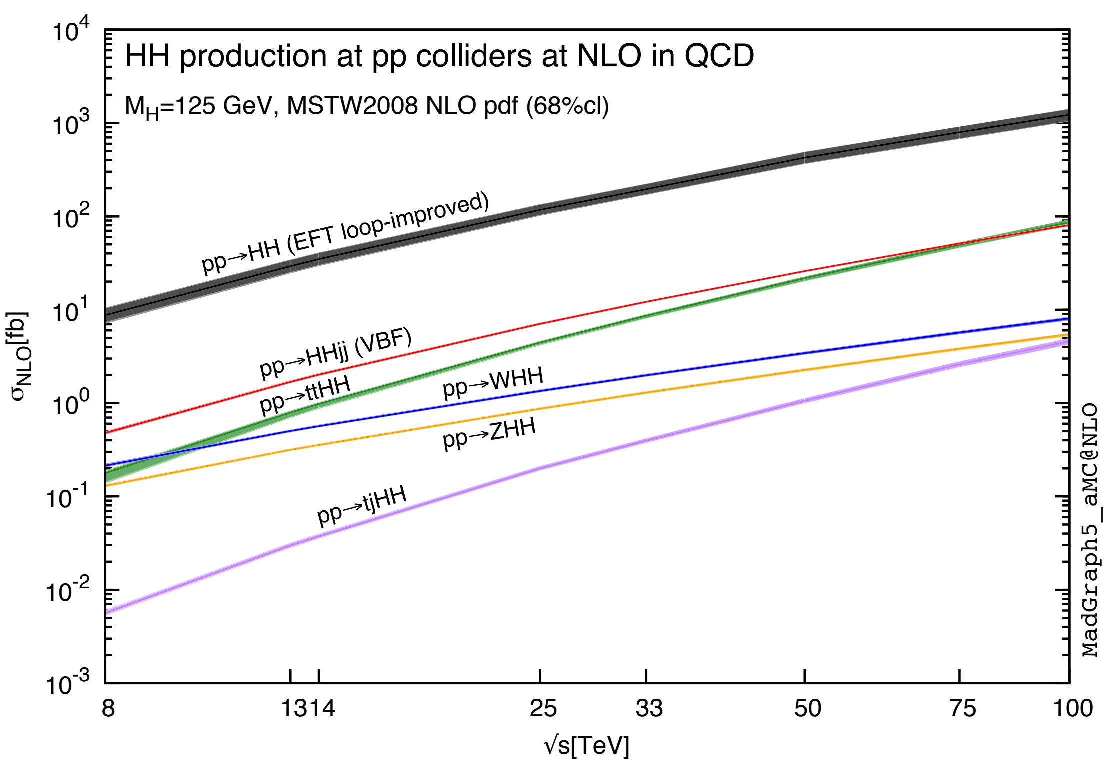

arxiv.org/abs/1401.7340v2

- CMS Future Studies 14 TeV results of
  - **HH→(bb̄)(γγ) shown**
  - **HH→(WW)(bb) shown**
  - HH→($\tau\tau$)(bb̄) and HH→(bb̄)(bb̄) under consideration

- **Run 1** HH→(bb̄)(γγ), HH→(bb̄)(bb̄) and HH→($\tau\tau$)(bb̄) in the works

Non-resonant HH→(ɣɣ)($b\bar{b}$) Future Study

- At **$\sqrt{s}$ = 14 TeV**, expected ~ **300 produced events** in 3 ab^{-1}
- Parametrized object performance tuned to **CMS Phase II detector at <PU> = 140**

Event selection:
- 2 photons: pT > 40 GeV and pT > 20 GeV, |η| < 2.5
- 2 b-tagged jets with CSV medium working point, pT > 30 GeV, |η| < 2.4
- Less than 4 jets with |η| < 2.4 and pT > 30 GeV
- Additional lepton veto
- Two categories considered: a) both photons in barrel, b) one photon in endcap

2D likelihood fit signal extraction in $m_{b\bar{b}}$ vs $m_{\gamma\gamma}$
- Window 100 GeV < $m_{\gamma\gamma}$ < 150 GeV, 70 GeV < $m_{b\bar{b}}$ < 200 GeV

Process / Selection Stage	HH	ZH	$t\bar{t}H$	$b\bar{b}H$	$\gamma\gamma$+jets	γ+jets	jets	$t\bar{t}$
Object Selection & Fit Mass Window	22.8	29.6	178	6.3	2891	1616	292	113
Kinematic Selection	14.6	14.6	3.3	2.0	128	96.9	20	20
Mass Windows	9.9	3.3	1.5	0.8	8.5	6.3	1.1	1.1

Table 3: The expected event yields of the signal and background processes for 3000 fb^{-1} of integrated luminosity are shown at various stages of the cut-based selection for the both photons in the barrel region. Mass window cuts are 120 GeV to 130 GeV for $M_{\gamma\gamma}$ and 105 GeV to 145 GeV for M_{bb}. A large fit mass window, 100 GeV to 150 GeV for $M_{\gamma\gamma}$ and 70 GeV to 200 GeV for M_{bb}, is used for the likelihood fit analysis. The statistical uncertainties on the yields are of the order of percent or smaller.

$S/\sqrt{B}$ = 2.1

ECFA Results

Non-resonant HH→(γγ)($b\bar{b}$) Future Study

ECFA Results

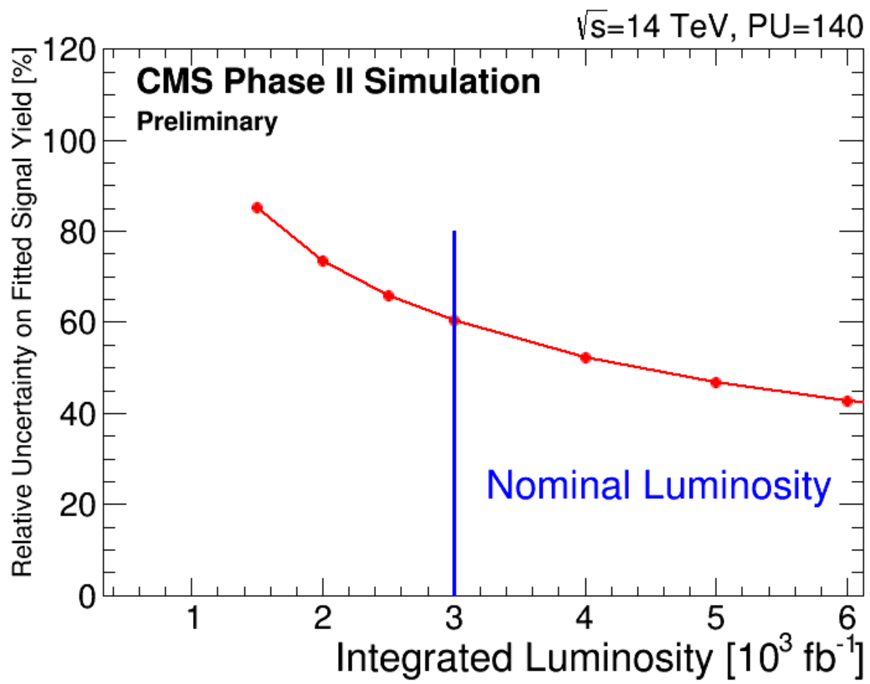

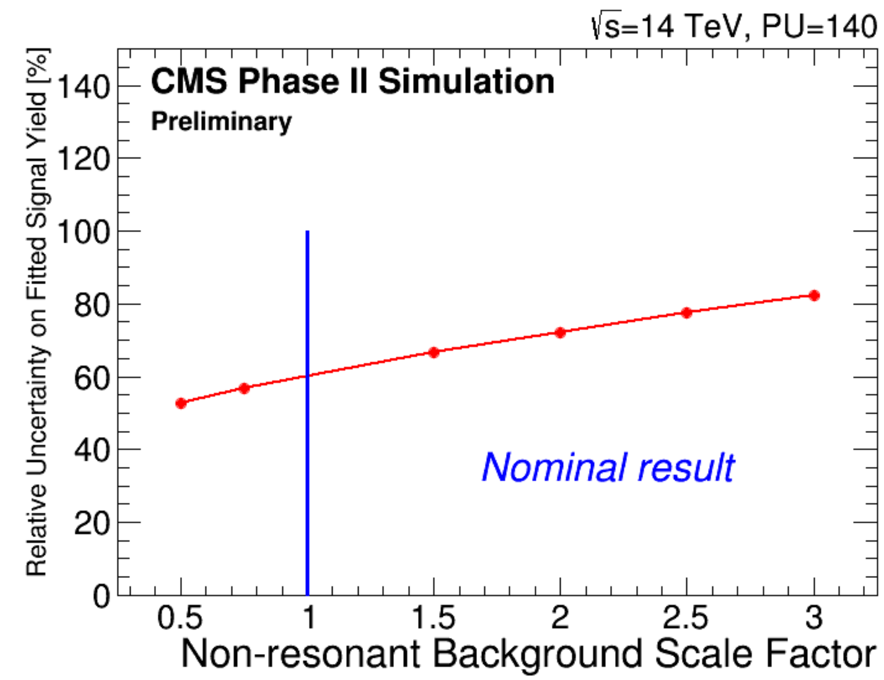

The **average expected relative uncertainty on the HH cross section** measurement as a function of integrated luminosity (top left), the scale factor for the non-resonant background (top-right), the b-tagging efficiency (bottom-left), and the photon efficiency (bottom-right)

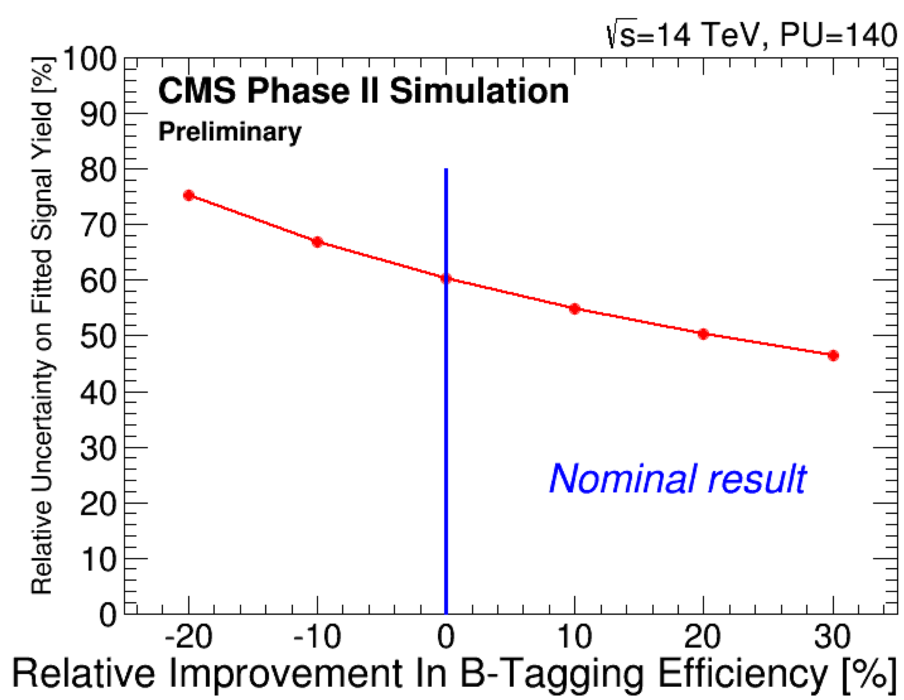

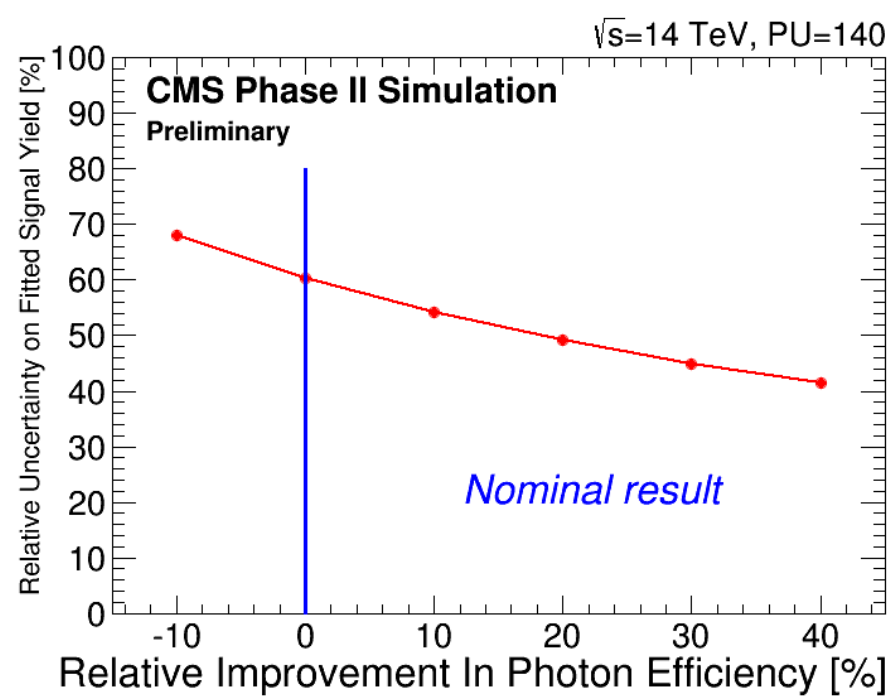

Non-resonant HH→(WW)(bb) Future Study

- At √s = **14 TeV**, expected **32000 produced events** in 3 ab^{-1}
- Delphes simulation of **CMS Phase II detector at <PU> = 140**
- Only main background tt considered.

Event selection:

- 2 leptons: mu pT > 20 GeV, e pT > 25 GeV
- 2 b-tagged jets with CSV medium working point, pT > 30 GeV, |η| < 2.4
- MET > 20 GeV

Neural Network Discriminant

- Variables M_{ll}, $M_{b\bar{b}}$, ΔR_{ll}, $\Delta R_{b\bar{b}}$, ΔR_{bl}, MET, $\Delta\phi_{b\bar{b}}$, $\Delta\phi_{ll}$, MT

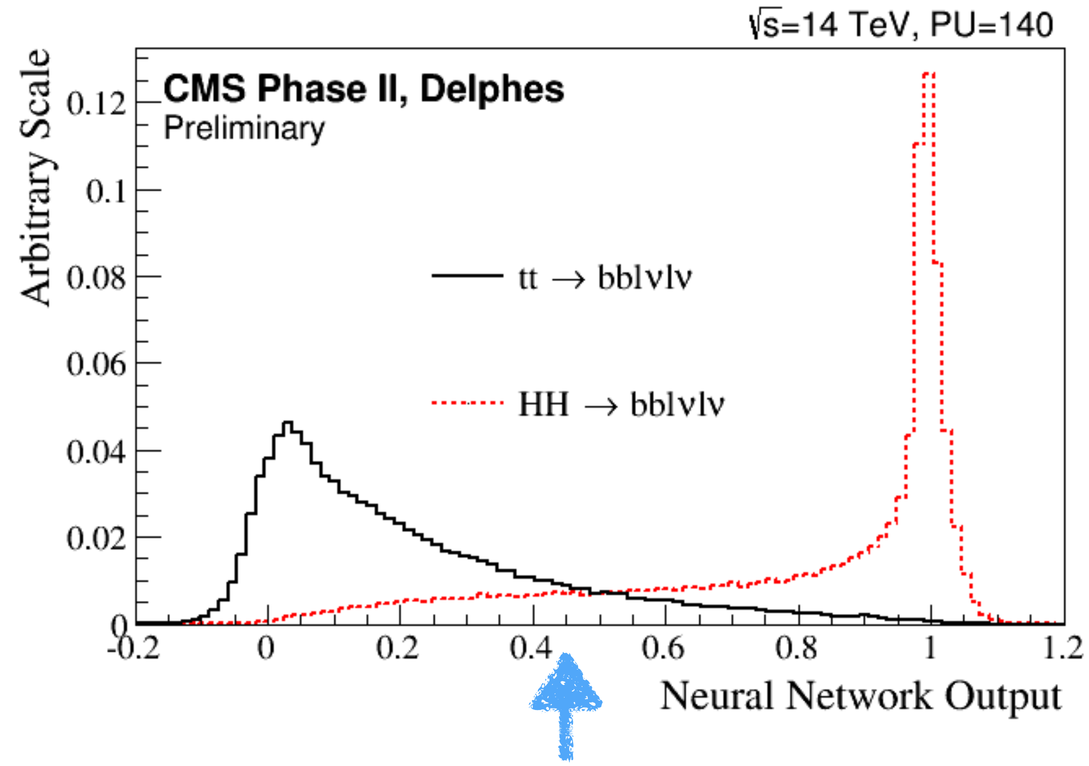

ANN discriminant, background tt peaking on low end, signal peaking on the high side. Signal region defined as events with ANN > 0.97

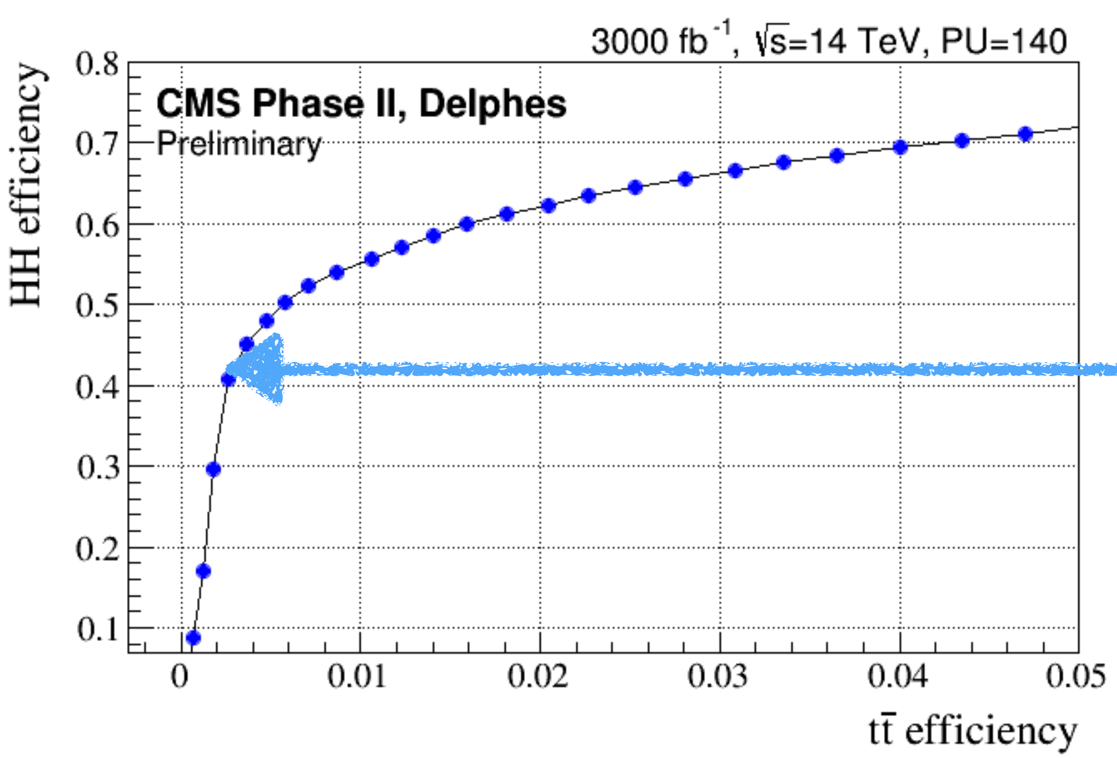

Signal (HH) eff. vs background eff. wrt ANN discriminant. Working point of ANN > 0.97 leads to 40% signal efficiency while rejecting 99.73% of the background

ECFA Results

Non-resonant HH→(WW)(bb) Future Study

ECFA Results

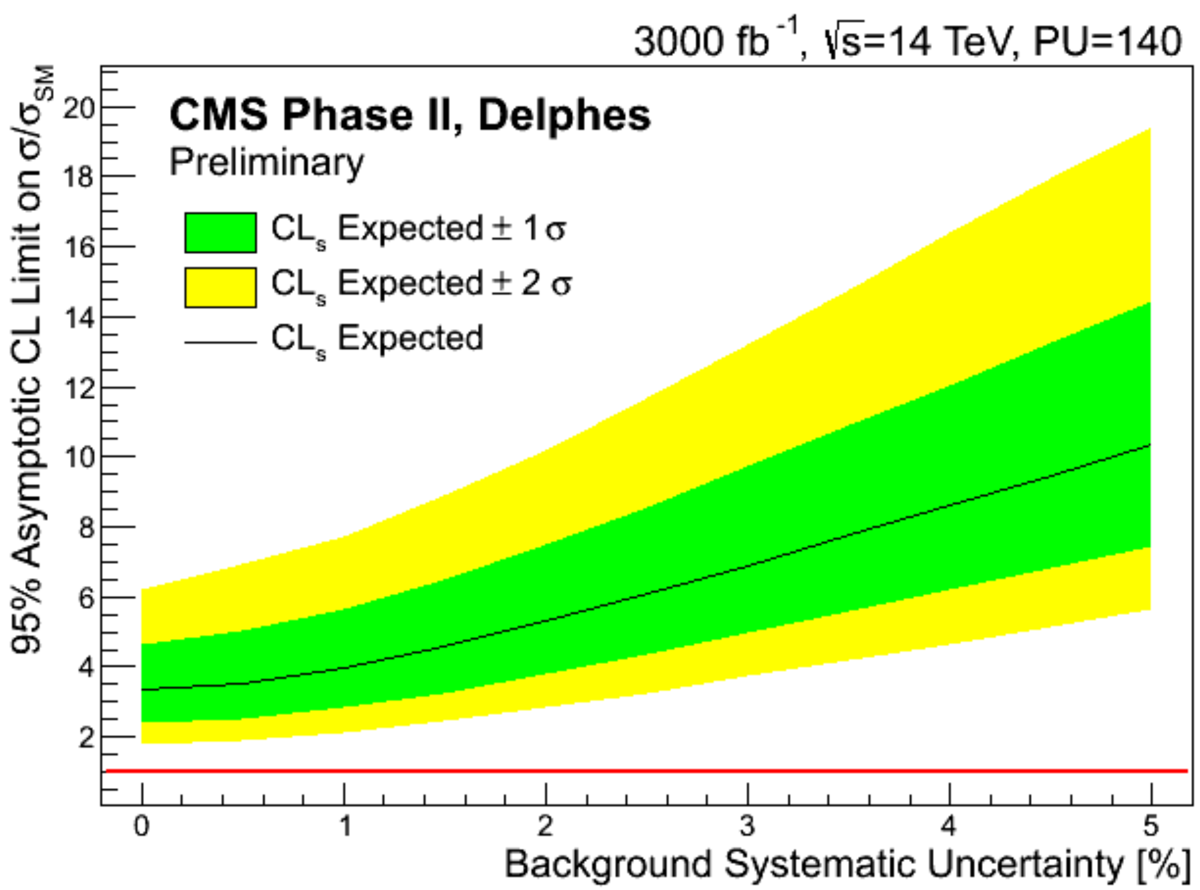

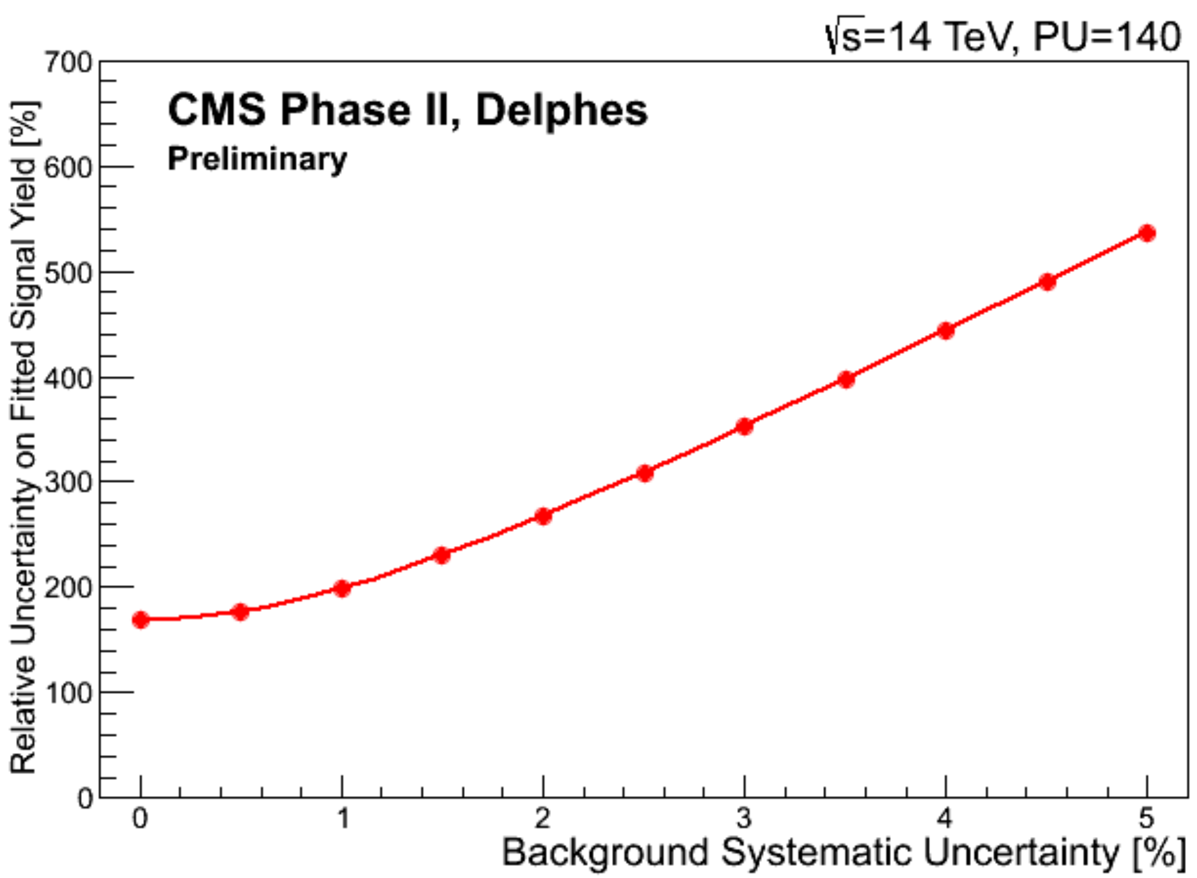

Expected 95% CL upper limits on the HH→(WW)(bb)→(ll)($\nu\nu$) production relative to SM expectation (left), and the average expected relative uncertainty on HH cross section (right), as a function of systematic uncertainty on background prediction. Data driven techniques expected to drive **uncertainties to the per cent level**.

Sensitive to ~ 3 to 10 x SM with 3 ab^{-1} of data.

$X \to HH \to (b\bar{b})(b\bar{b})$

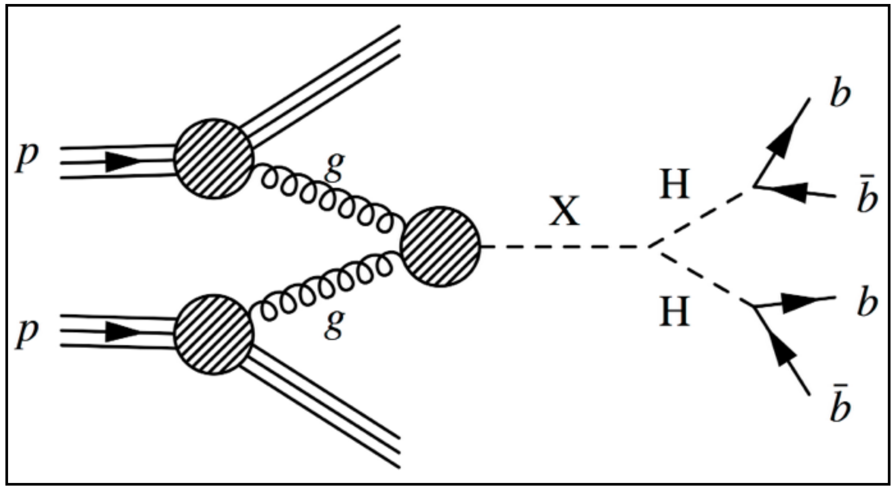

Signal

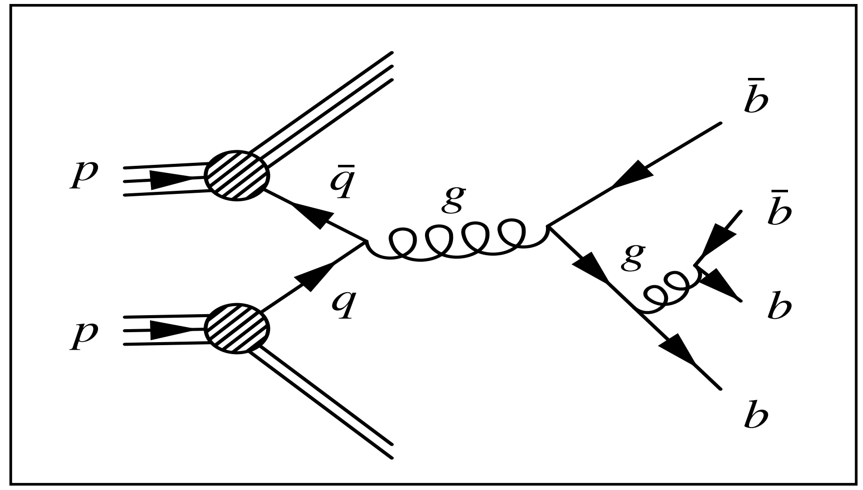

Example QCD multijet background diagram

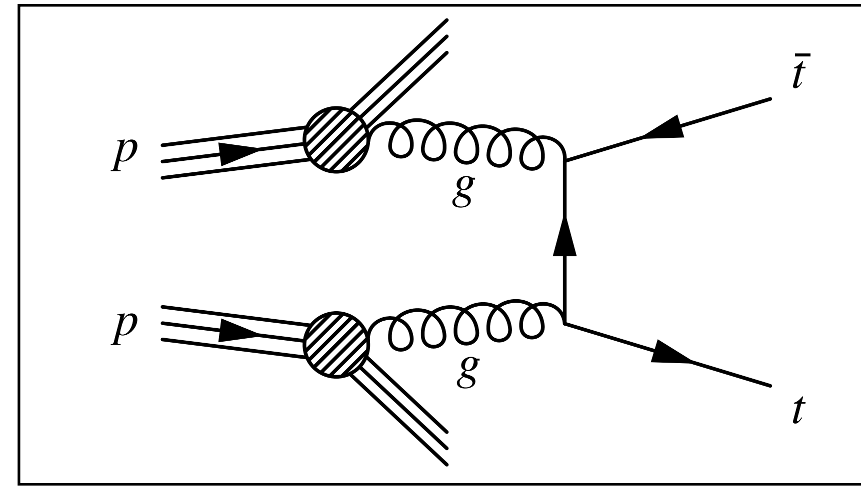

Example tt background diagram

Highest Higgs branching fraction to $b\bar{b}$. Have to unearth signal from under copious 4-jet **QCD multi-jet background**, which includes ~ 23% of $t\bar{t}$. We exploit:

- **Resonant structure of signal** over relatively smooth background in m_X
- **Signal shape modeled from MC**, where *X* is a radion
- Background decomposed into two components
    - **$t\bar{t}$ component**. Parametric form from MC
    - **QCD multi-jet component**. Form modeled from data sidebands, validated in several Control Regions

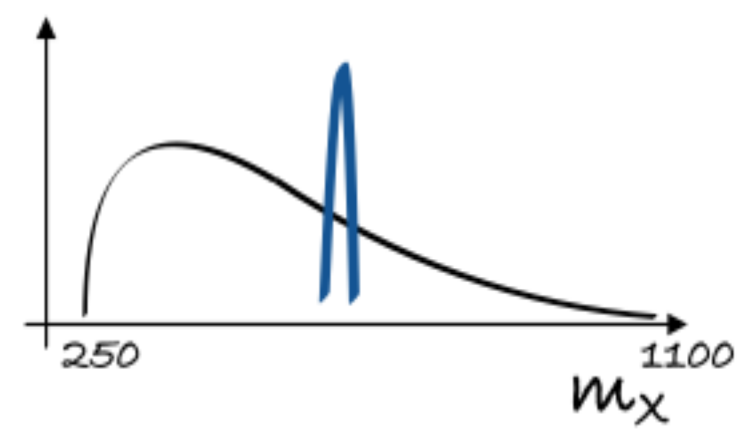

- b-tagging at the **trigger**
- **Powerful offline b-tagging** (CMVA algorithm) with 75% b-tagging and 3% mistagging efficiency
- Good **$m_{b\bar{b}}$ resolution** for a sharp signal peak
- Further enhanced by **kinematic constraint** on jet energies to the Higgs mass
- Conducted in **two mass regimes**:
  Low Mass Regime: 270 GeV ≤ mX ≤ 450 GeV, *High Mass Regime*: 450 GeV < mX ≤ 1100 GeV

X→HH→(b$\bar{b}$)(b$\bar{b}$): QCD Background Modeling

All-hadronic final state **dominated by multi-jet QCD**. Cannot rely on MC. **Functional form** from studying data.

Signal Region (SR) defined in (m_{H1}, m_{H2}) plane

$\Delta m^2_{H1} + \Delta m^2_{H1} < (17.5\text{ GeV})^2$ where $\Delta m_{H1,2} = m_{H1,2} - 125$ GeV

We cannot look in here. Blind Analysis.

Sideband Region (SB) defined as

$(35\text{ GeV})^2 < \Delta m^2_{H1} + \Delta m^2_{H1} < (17.5\text{ GeV})^2$

and $\Delta m_{H1} \Delta m_{H2} < 0$

Validation Region (VR) and Validation Region Sideband (VB) centered around (90 GeV, 90 GeV)

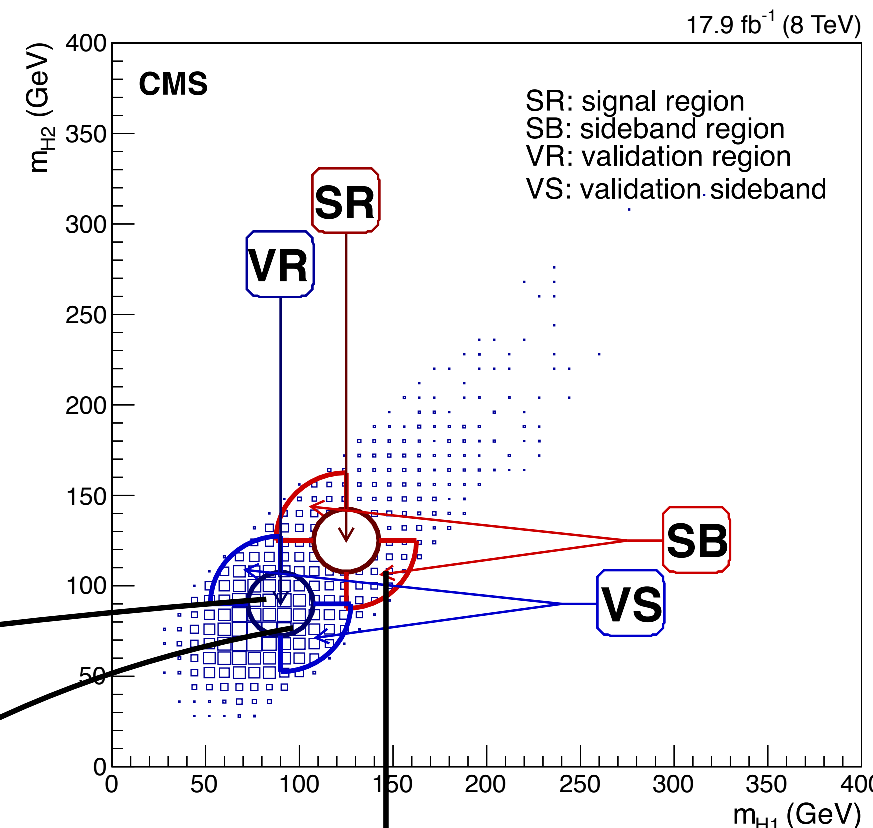

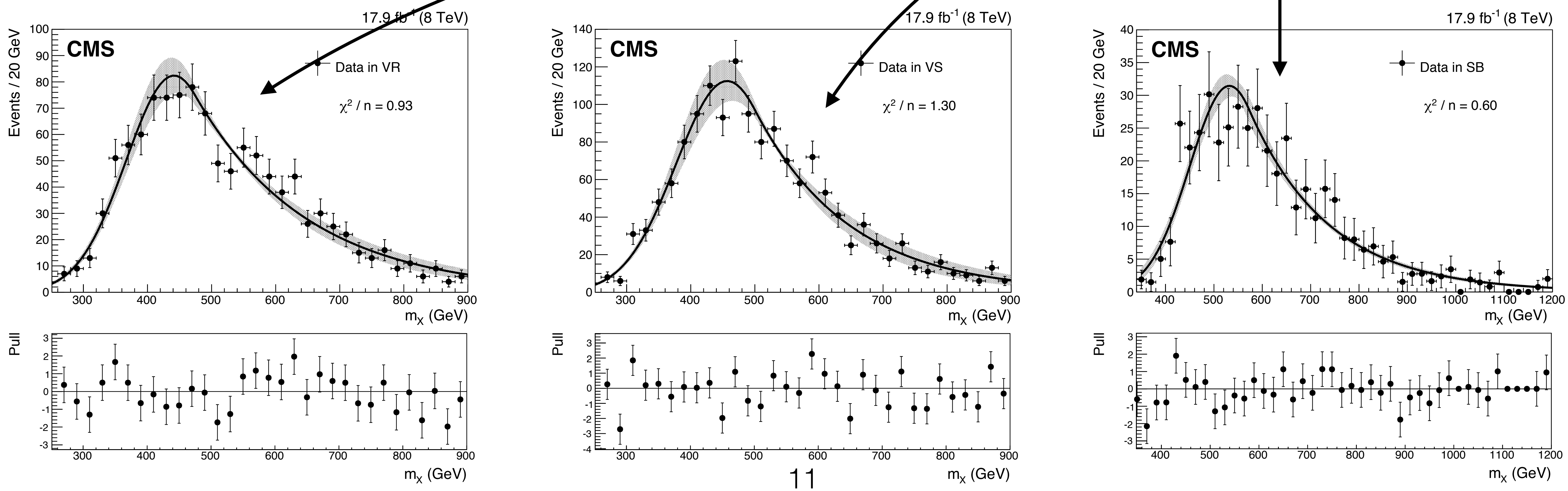

X→HH→(bb̄)(bb̄): Results

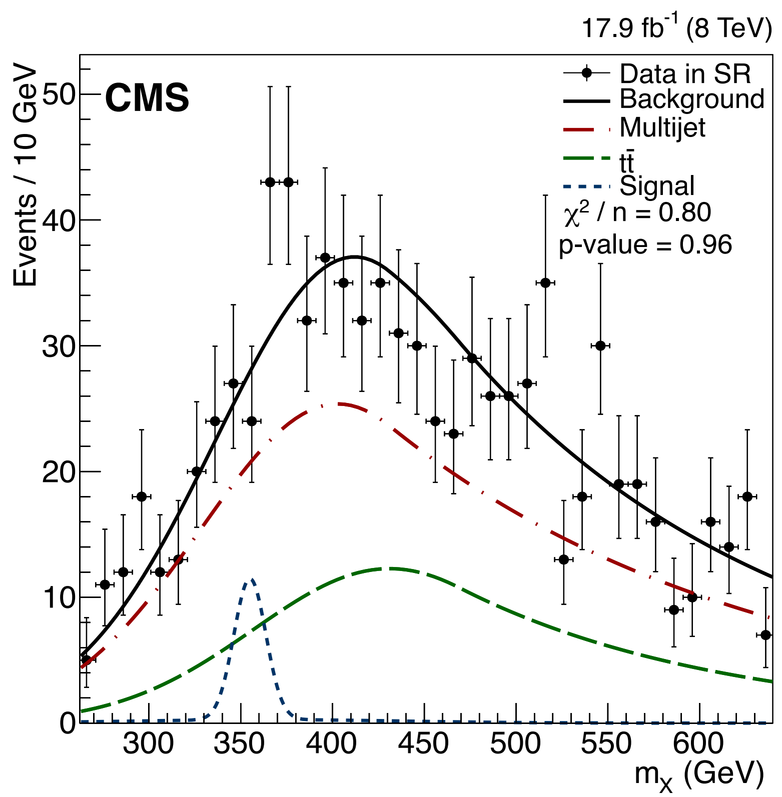

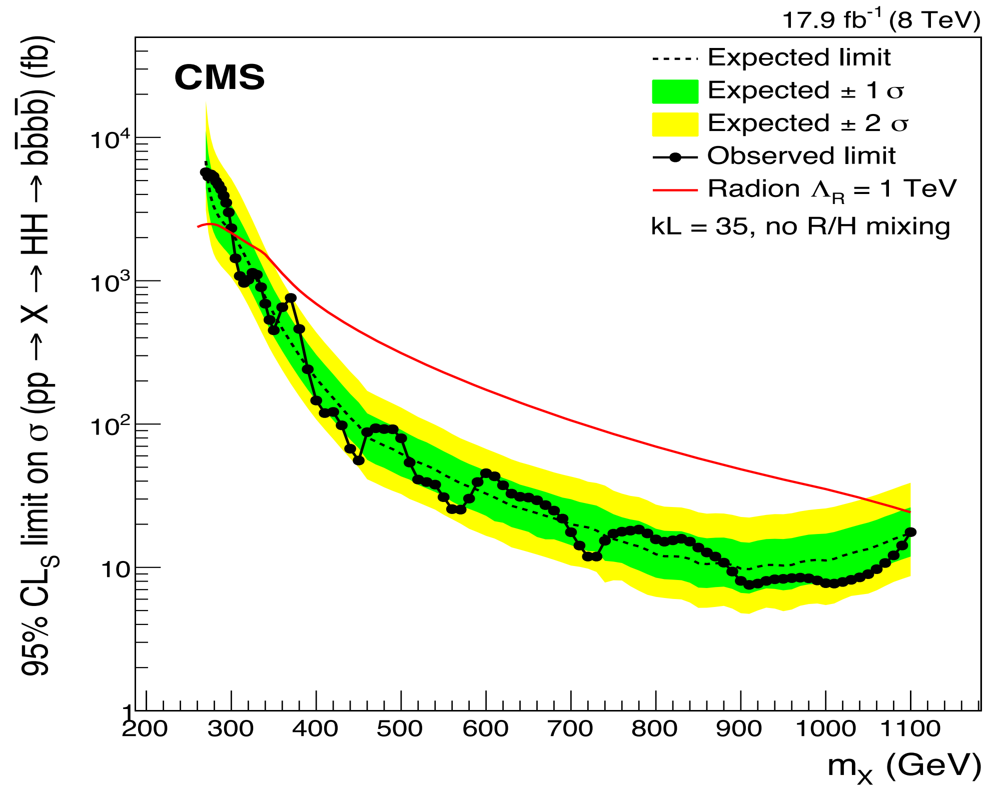

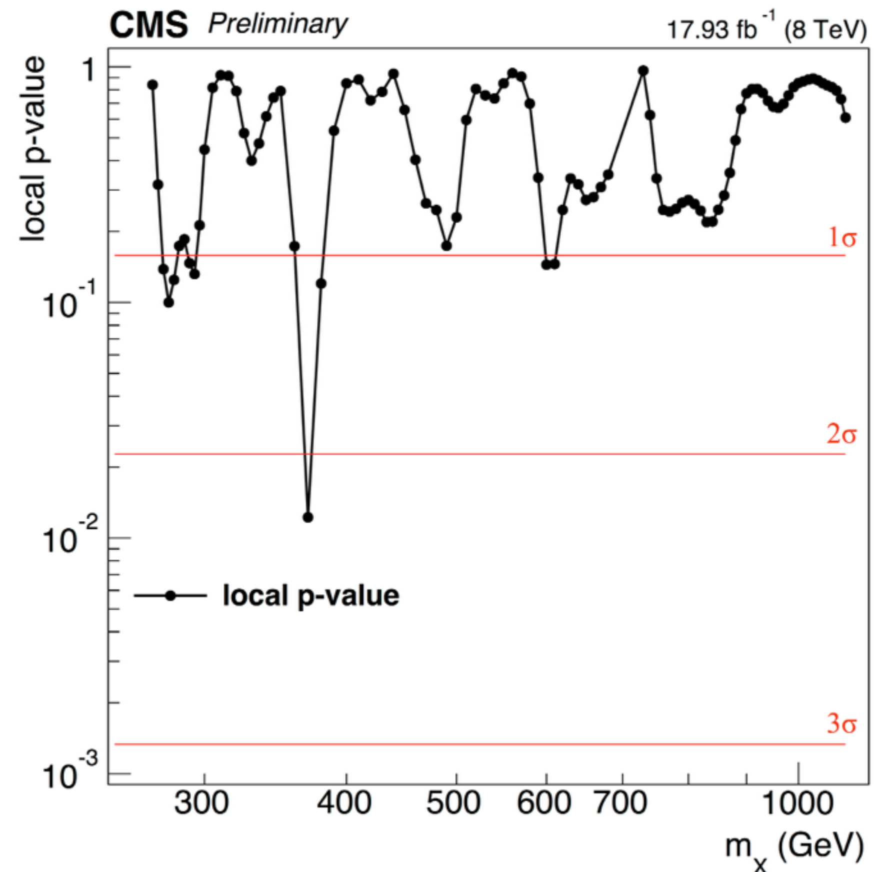

No significant deviation from expectations

- Maximum excess has local p-value of 2.1σ, global p-value of 1σ. **No significant excess** and no significant deviation from expected limits.
- **Recent result**. Being reviewed at **PLB**. http://arxiv.org/abs/1503.04114.
  Twiki: https://twiki.cern.ch/twiki/bin/view/CMSPublic/Hig14013PaperTWiki
- The **RS1 radion** in WED scenario kL = 35, right handed top on EWK brane, no radion-Higgs mixing, with Λ_R = 1 TeV is excluded between 300 and 1.1 TeV. The first excitation of **KK-graviton** in same scenario excluded from 380 to 830 GeV at a 95% CL. Br(R→HH) = 0.25 is assumed.

$X \rightarrow HH \rightarrow (b\bar{b})(\gamma\gamma)$

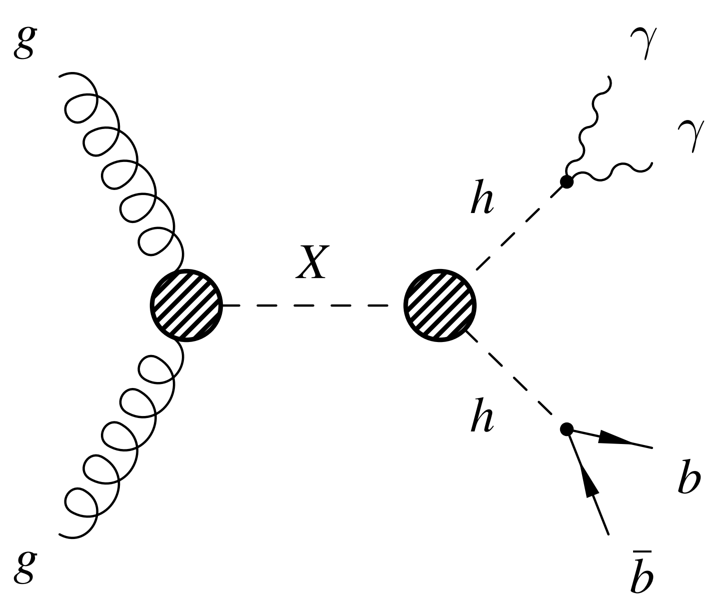

- This channel has a lower branching fraction (0.26%), but also lower QCD multi-jet background. We exploit:
  - High efficiency to reconstruct photons (>90%)
  - Sharp H(γγ) resolution
  - Three invariant mass handles: $m_{\gamma\gamma}$, m_{jj}, $m_{\gamma\gamma jj}$
- Two **di-photon triggers** [used by H(γγ) analysis] used to collect data.
- **Two mass regimes** of the analysis:
  - Low Mass Regime: 260 GeV ≤ mX ≤ 400 GeV
  - High Mass Regime: 400 GeV < mX ≤ 1100 GeV
- Each regime analyzed in **two purity categories**:
  - Medium purity: 1 b-tagged jet
  - High purity: 2 b-tagged jets

Photon Object Selection

- Tight photon identification
- Sliding pT cuts:
  - $p_{T\gamma 1}/m_{\gamma\gamma} > 1/3$
  - $p_{T\gamma 2}/m_{\gamma\gamma} > 1/4$
- $|\eta_\gamma| < 2.5$
- 100 GeV < $m_{\gamma\gamma}$ < 180 GeV

b-jet Object Selection

- Loose jet identification
- Pileup rejection
- $p_{Tj} > 25$ GeV
- $|\eta_j| < 2.5$
- Combined Secondary Vertex. b-tag eff = 70%, mistag rate = 1-2%

$X \rightarrow HH \rightarrow (b\bar{b})(\gamma\gamma)$

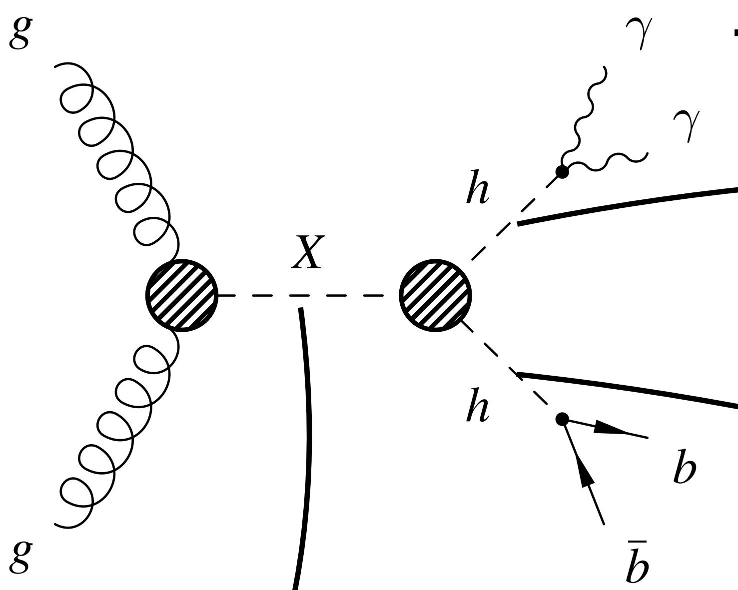

Three invariant mass handles $m_{\gamma\gamma}$, m_{jj}, $m_{\gamma\gamma jj}$

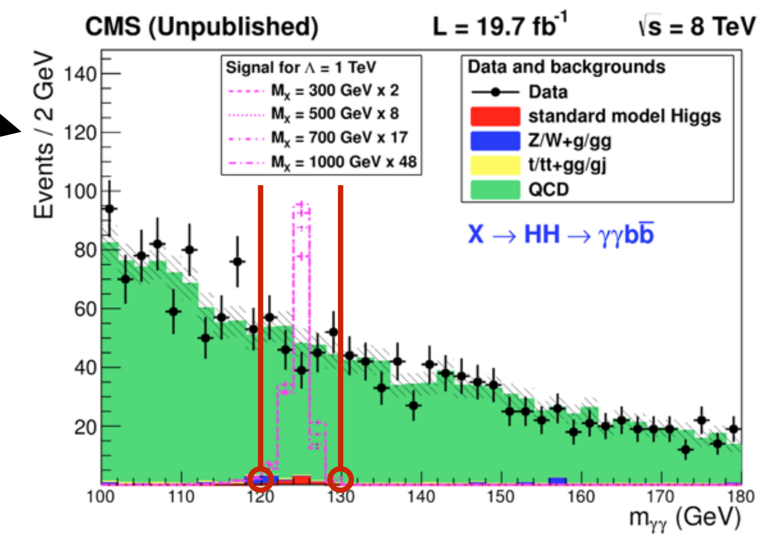

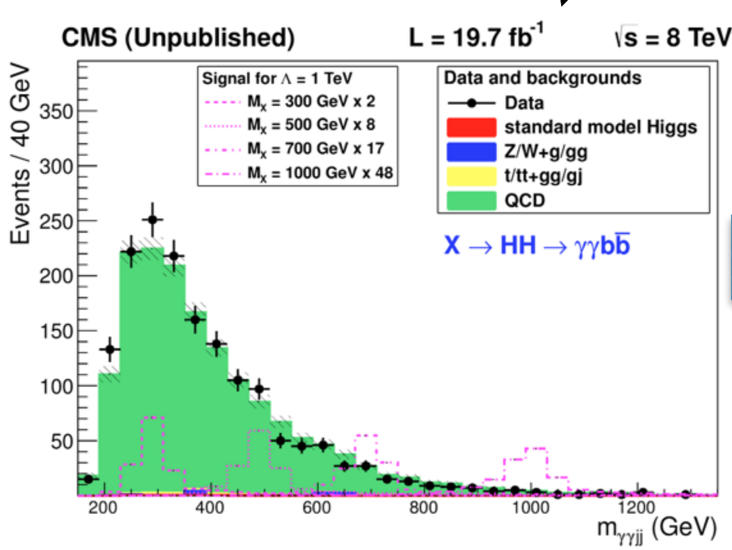

Kinematic Fit

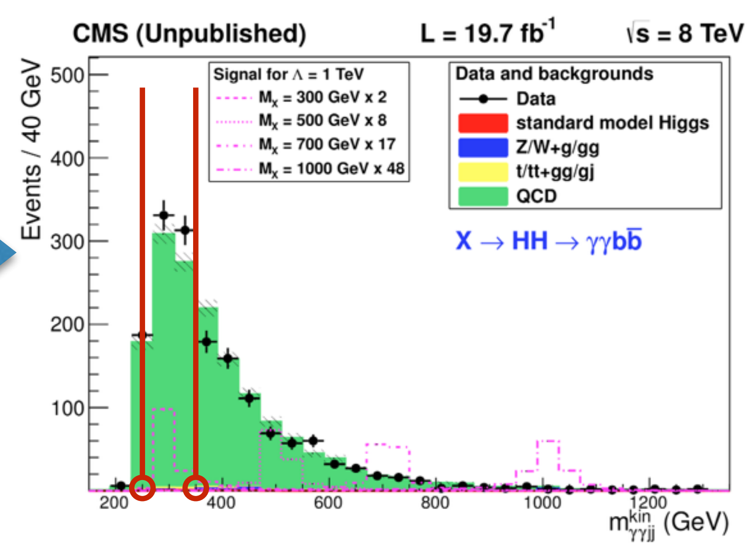

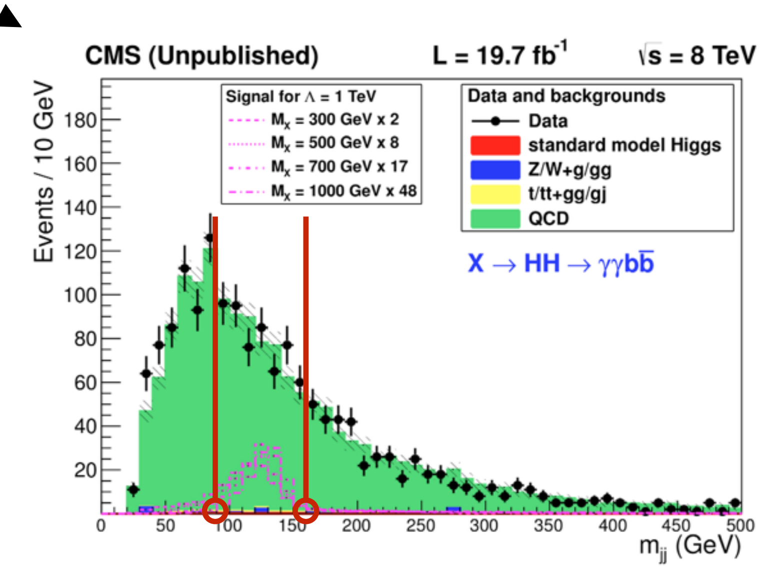

Low Mass Regime.

- Cut on $m_{\gamma\gamma jj}$ AND m_{jj}.
- Fit $m_{\gamma\gamma}$

High Mass Regime

- Cut on $m_{\gamma\gamma}$ AND m_{jj}.
- Kinematically constrain $m_{\gamma\gamma}$ and m_{jj} to 125 GeV within energy resolutions
- Fit $m_{\gamma\gamma jj}$

$X \to HH \to (b\bar{b})(\gamma\gamma)$: Results

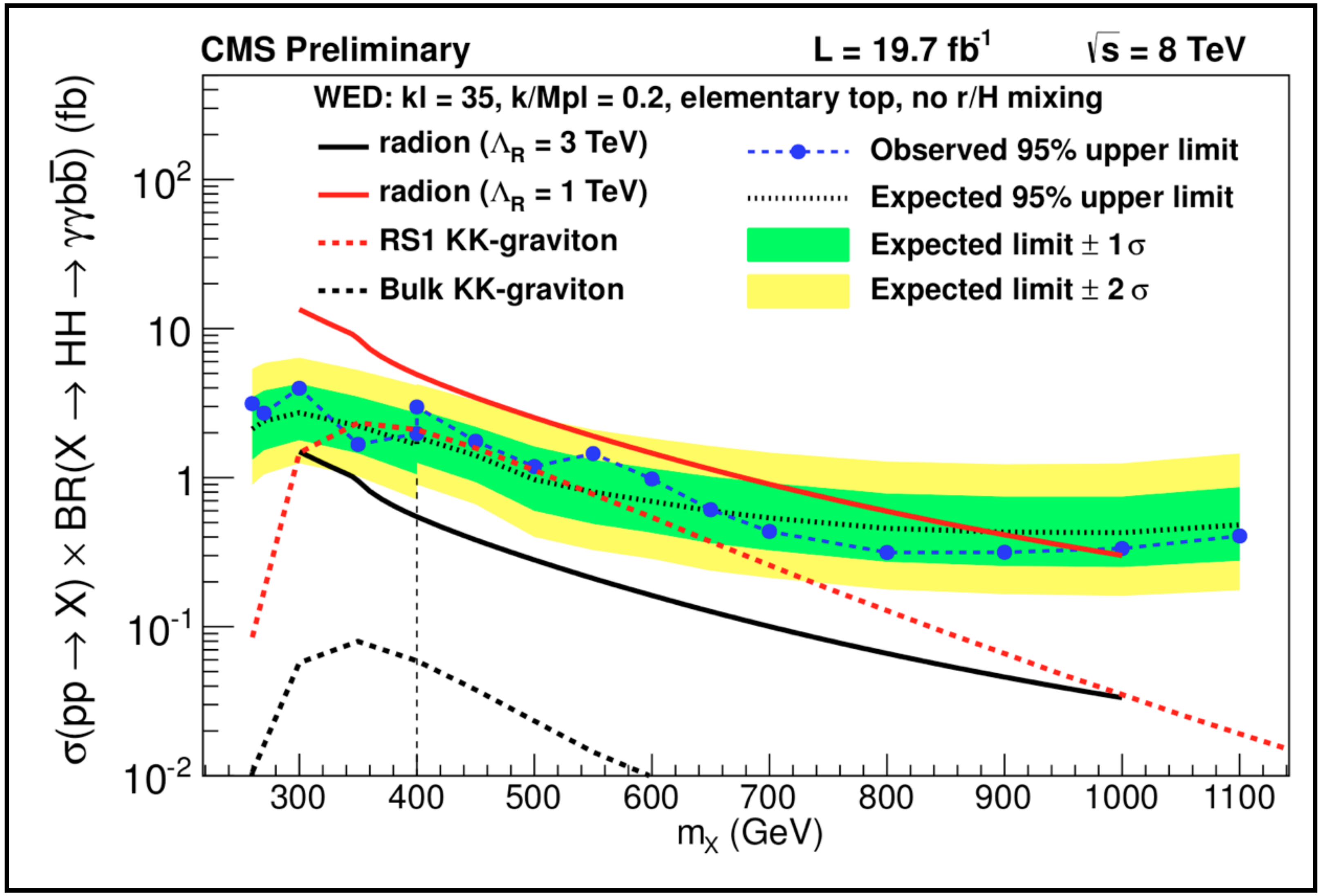

No significant deviation from expectations

- The **RS1 radion** with Λ_R = 1 TeV is excluded below 970 GeV. The **KK-graviton** is excluded from 340 to 400 GeV at a 95% CL.
- Public results available here: CMS-HIG-13-032

HH→(ll)(ll/ɣ)

Multiple final states considered

	$h \to WW^*$	$h \to ZZ^*$	$h \to \tau\tau$	$h \to bb$	$h \to \gamma\gamma$
$h \to WW^*$	✓	✓	✓	X	✓
$h \to ZZ^*$	-	✓	✓	✓	✓
$h \to \tau\tau$	-	-	✓	X	✓
$h \to bb$	-	-	-	X	X
$h \to \gamma\gamma$	-	-	-	-	X

Final states from hh decays	Search Channels h decays populate
WW^*WW^* $WW^*\tau\tau$ $\tau\tau\tau\tau$ $ZZ^*\tau\tau$ ZZ^*bb	Three or four leptons (upto one τ_h), OSSF pair off-Z or no OSSF pair in bins of E_T^{miss} and b-tag
$\gamma\gamma WW^*$ $\gamma\gamma ZZ^*$ $\gamma\gamma\tau\tau$	2photons ($M_{\gamma\gamma}$ within higgs bin) + 1 or more leptons(upto 2 τ_h),in bins of E_T^{miss}

Multiple lepton requirement cuts down QCD. Cut and count analysis performed

- **di-photon and di-lepton triggers** used
- Final states classified by:
  N_l, opposite-sign-same-flavor (OSSF) pairs, on/off-Z, N_γ, N_τ, N_b, E_T^{miss}
- Multi-lepton channels contributing the most:
  - Channels **without OSSF**-pair (greatly reduces DY-background)
  - Channels with OSSF-pair but **off-shell Z**
  - Channels with **SSSF-pair**. Has low SM background

HH→(ll)(ll/ɣ): Results

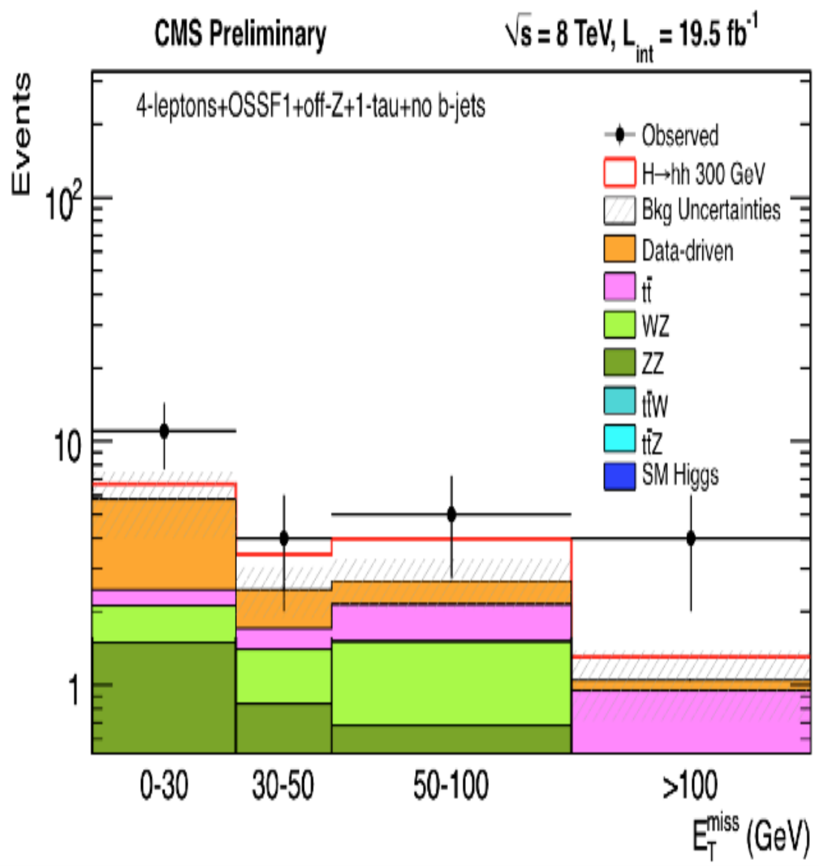

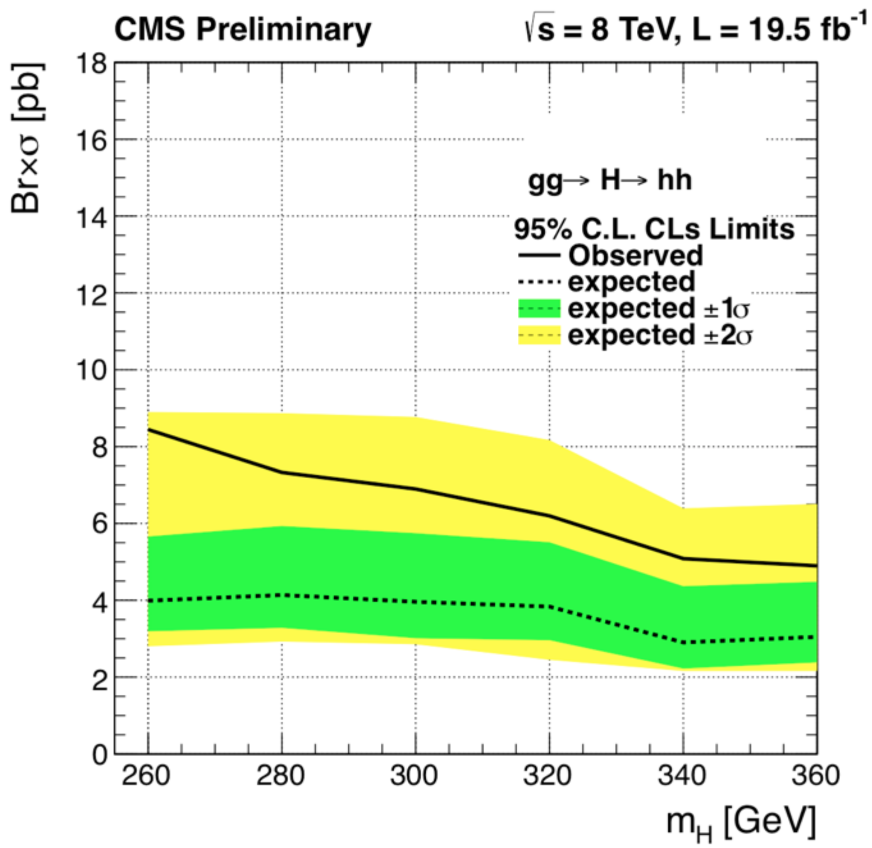

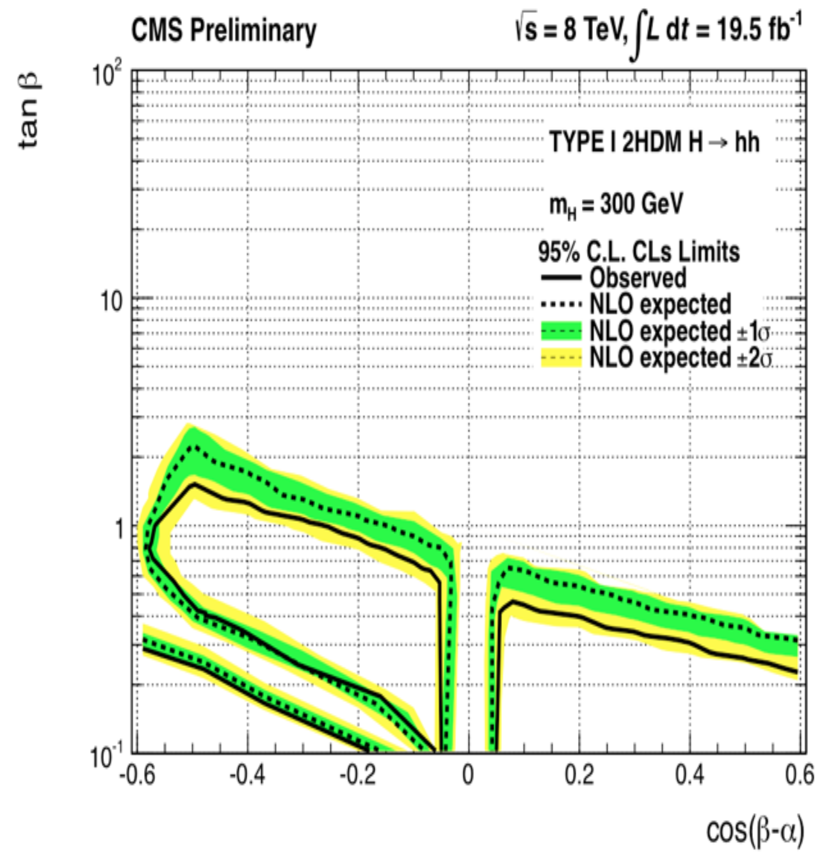

Signal bin with largest excess in 4-leptons, OSSF1, off-Z, 1 τ_{had} and 0 b-jets.

Total excess:
obs (exp) = 20 (10.7 ±1.9)

Local significance ***p* = 1.5%**
40 channels significance: ***p* = 46%**

Observed and expected limits for **σ**(gg→H→hh). Standard Model branching fractions are assumed for the Higgs.

No significant deviation from expectations

Interpret limits on **σ**(gg→H→hh) in Type I 2HDM parameter space

Regions below the curves and within the loops **are excluded**

Combined Run 1 di-Higgs results

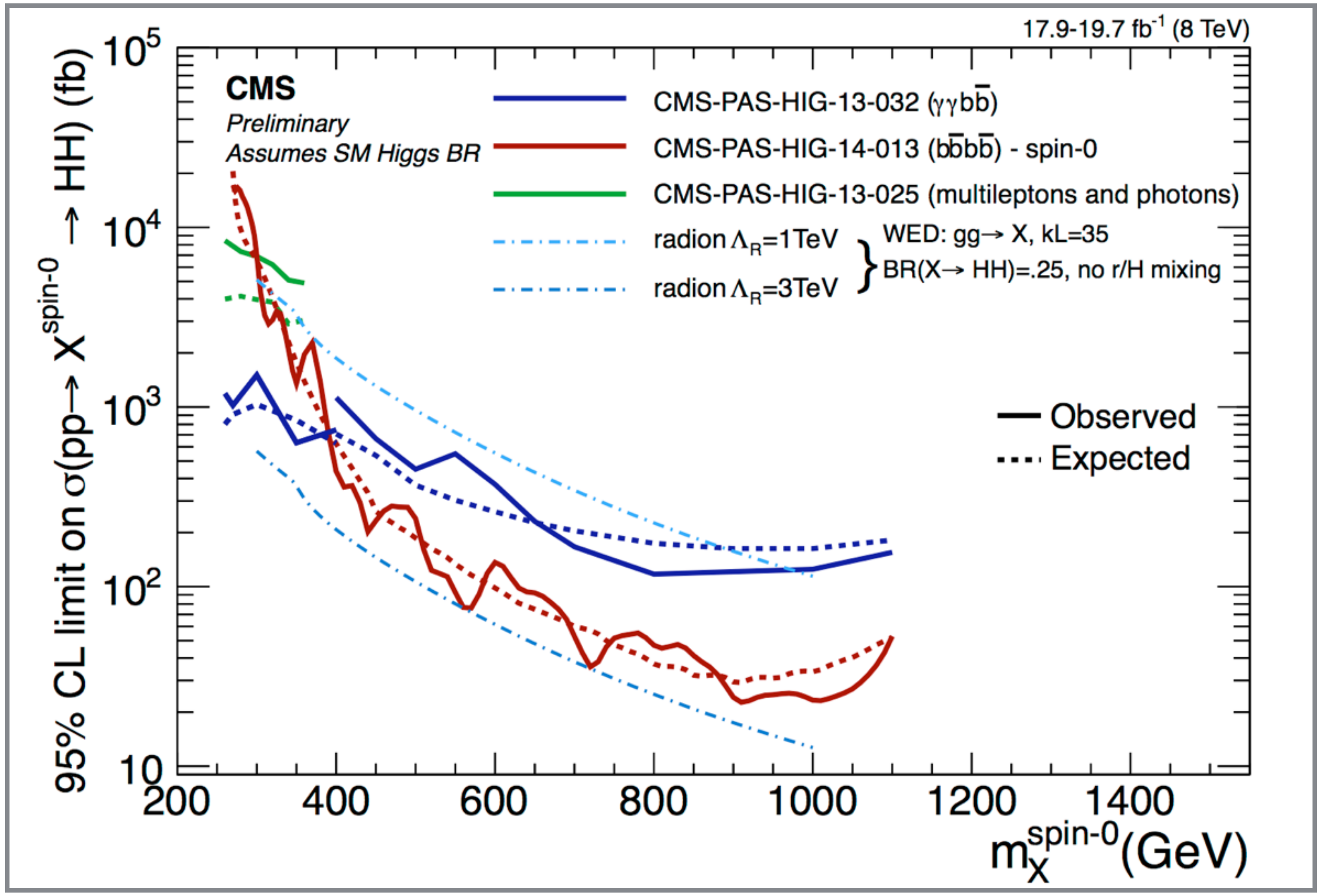

No significant deviation from expectations

- X→H(γγ)H($b\bar{b}$) and X→H($b\bar{b}$)H($b\bar{b}$) sensitivities cross. **Complementary searches**.
- Resonant searches **constrain Beyond the Standard Model Physics**: 2HDM and WED (RS1)
- New Run 1 analysis for **X→HH→($\tau\tau$)($b\bar{b}$)** also underway.

X→HH→(b$\bar{b}$)(b$\bar{b}$): Prospects

Run 1

Boosted HH→(b$\bar{b}$)(b$\bar{b}$)

- We analyze merged jets
- Use jet substructure to b-tag
- Overlap in mX range with unboosted analysis. Can extend our search range up to ~ 3 TeV.

Work ongoing

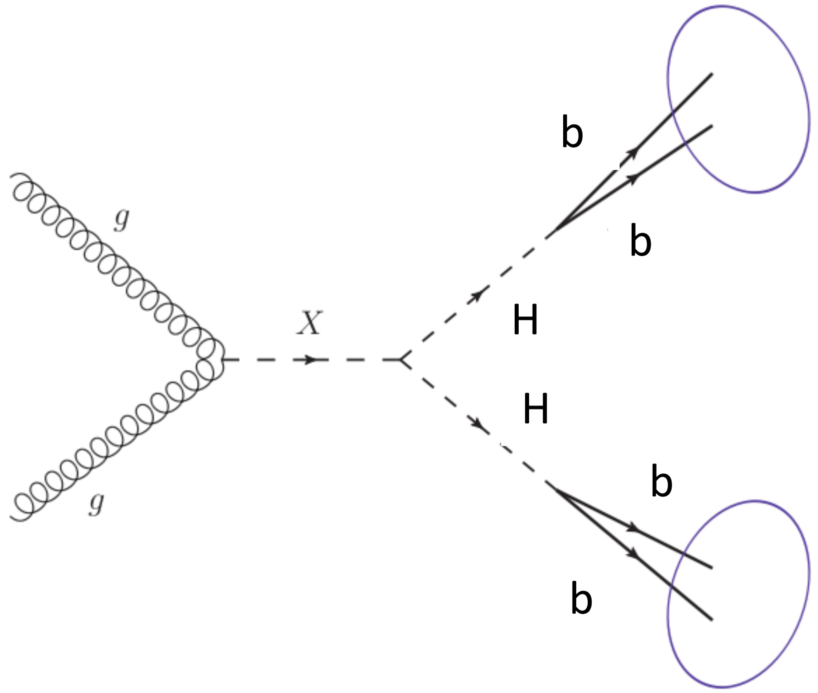

X→HH→($b\bar{b}$)($b\bar{b}$): Prospects

Run 2

HH→($b\bar{b}$)($b\bar{b}$)

- **Better designed triggers** in place. Run 1 triggers were designed for a Z($b\bar{b}$)H($b\bar{b}$) search!
- **AK4 jets** instead of AK5 jets will allow us to go further without substructure
- We can probe **non-negligible resonance widths**, thus offering 2HDM exclusion
- QCD multijet 4 b-jet cross section increases 7 fold for $\sqrt{s}$ going from 8 TeV→ 13 TeV. (http://arxiv.org/pdf/1410.2794.pdf). $t\bar{t}$ cross section increases 3 fold.
- However, **theoretical cross sections of all signals grow** at least by the parton luminosity ratio of 3 - 10
- What theories other than WED and 2HDM can we probe?

Work ongoing

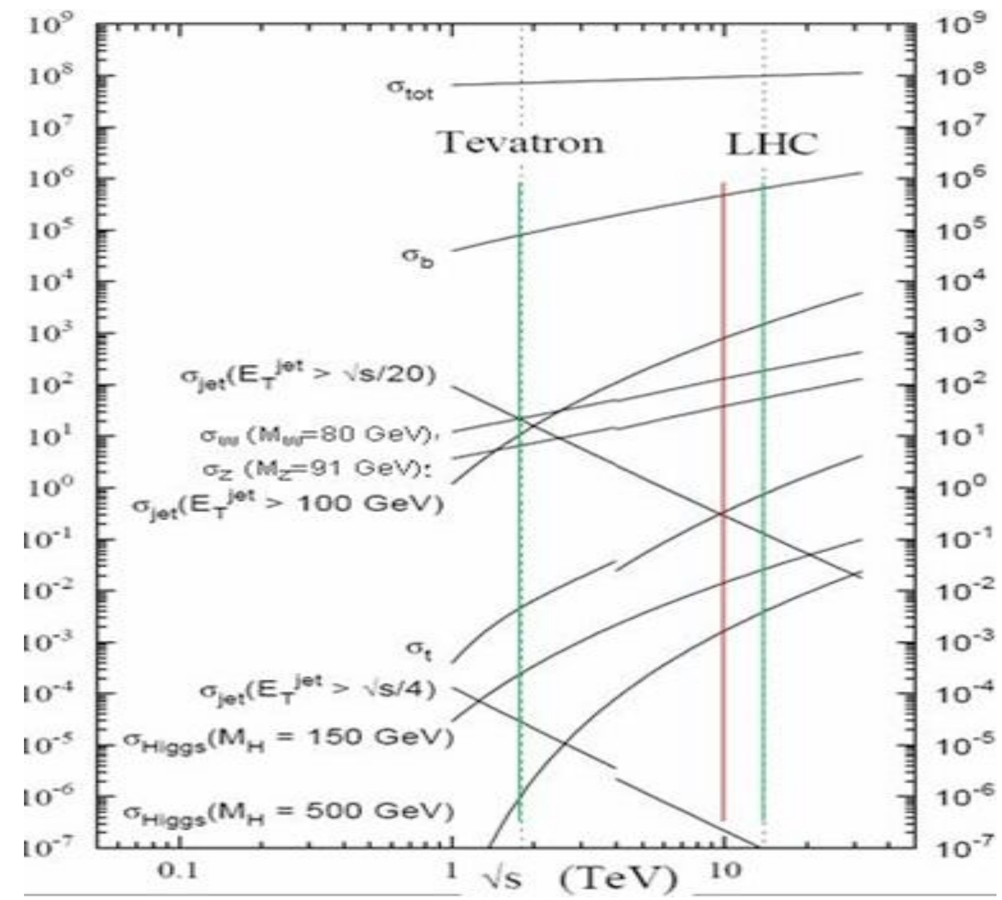

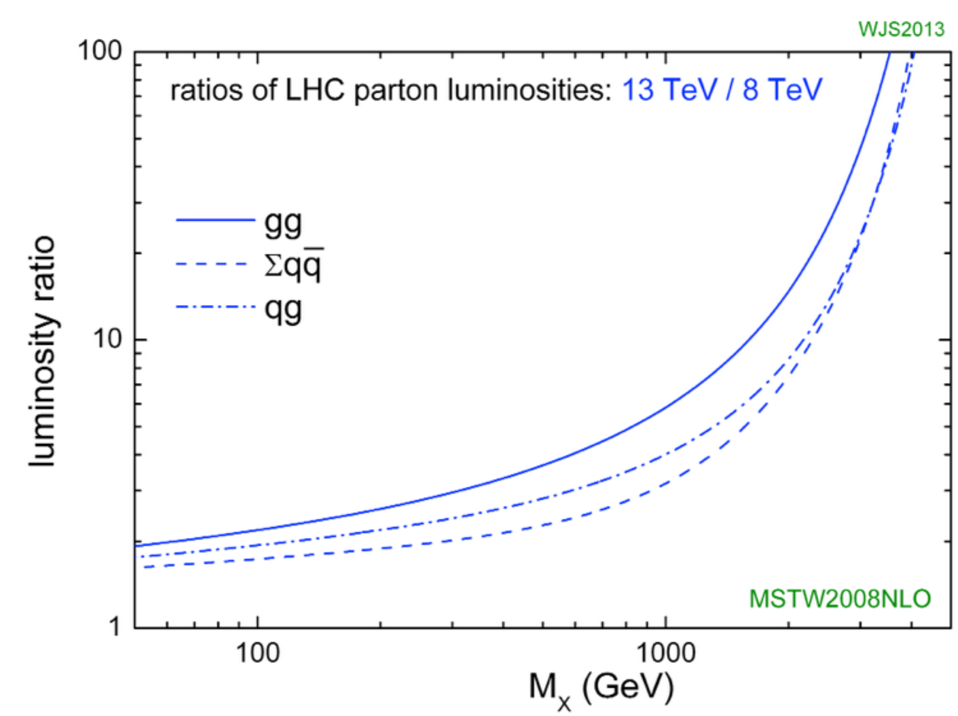

Conclusions

- CMS future studies indicate sensitivities < 10 x SM with 3 ab^{-1} of data at 14 TeV using the H(WW)H(bb) channel
- Non-resonant HH studies for Run 1 are underway

- CMS has **Run 1 results for resonant** Higgs pair production at 8 TeV. No statistically significant signal observed. Interpreted as **exclusions for WED and 2HDM** parameter space.
- We will cast a **wider net in Run 2** for resonant searches
  - Non-negligible resonance width
  - m_H not constrained to 125 GeV, but scanned
  - Will use jet substructure Higgs-tagging tools

Higgs pair-production hunters are now a vibrant community within CMS

BACKUP

Multi-lepton and Photons: Systematics

Source of Uncertainty	Uncertainty
Luminosity	2.6%
PDF	10%
$E_{\mathrm{T}}^{\mathrm{miss}}$ Resolution/Smearing: 0-50 GeV, 50-100 GeV, >100 GeV	(-3%, +4%, +4%)
Jet Energy Scale	0.5%
B-Tag scale factor	0.1% (WZ), 6% ($t\bar{t}$)
Muon ID/Isolation at 30 GeV	0.2%
Electron ID/Isolation at 30 GeV	0.6%
Trigger Efficiency	5%
$t\bar{t}$ xsec	10%
$t\bar{t}$ fake rate contribution	50%
WZ cross-section	15%
ZZ cross-section	15%

Table 6: The systematic uncertainties associated with this analysis. The $E_{\mathrm{T}}^{\mathrm{miss}}$ resolution systematic is given for WZ background on Z for different cuts on $E_{\mathrm{T}}^{\mathrm{miss}}$ and for different cuts on M_T given a cut of $E_{\mathrm{T}}^{\mathrm{miss}} > 50$ GeV.

Multi-leptons and Photons: Background Estimation

Multi-lepton final states

- **Z+jets**, **W+jets**. Data-driven estimation (of jets misidentified as leptons)
- **$t\bar{t}$ and VV**: MC-based estimation
- **Asymmetric photon conversion**. DY process with one soft lepton and another lepton radiating a photon that converts. Data-driven estimation of photon conversion.

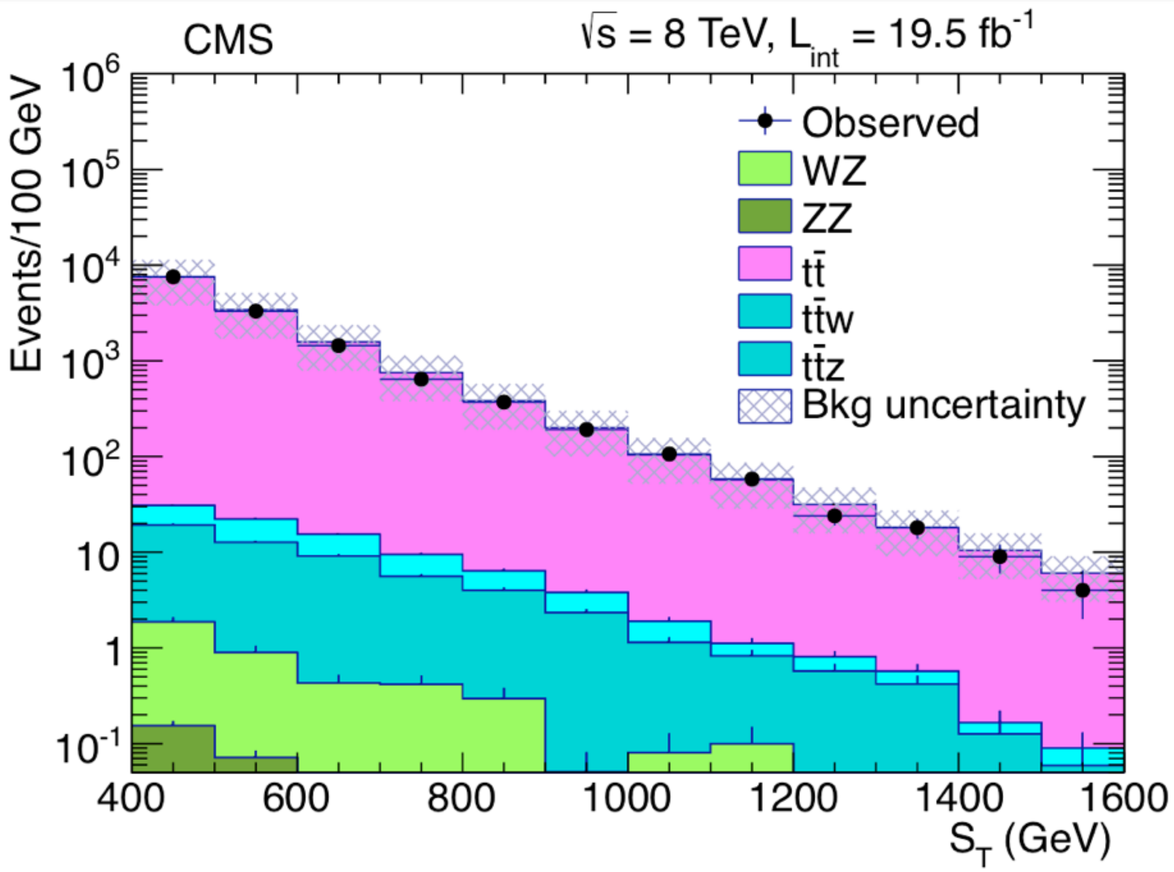

Di-photon final states

- Background estimated from $m_{\gamma\gamma}$ sidebands keeping the range 120 GeV — 130 GeV blinded.
- Fitted to a falling exponential

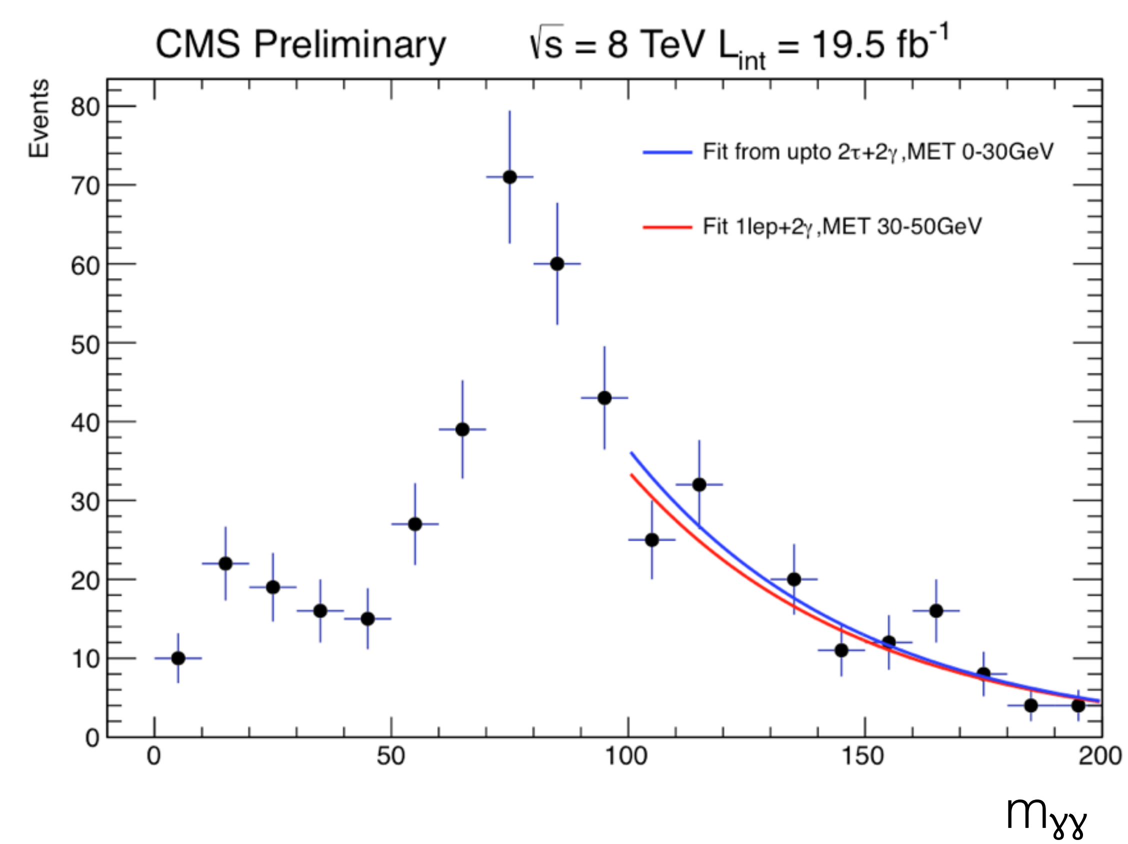

Multi-lepton and Photons: Event Counts

4 Lepton Results										
Selection	on- or off-Z	E_T^{miss}	N_τ=0, N_{b-Jet}=0		N_τ=1, N_{b-Jet}=0		N_τ=0, $N_{b-Jet}\geq1$		N_τ=1, $N_{b-Jet}\geq1$	
			obs	expect	obs	expect	obs	expect	obs	expect
OSSF0	NA	(100,∞)	0	0.07 ± 0.07	0	0.18 ± 0.09	0	0.05 ± 0.05	0	0.16 ± 0.1
OSSF0	NA	(50,100)	0	0.07 ± 0.06	2	0.8 ± 0.35	0	0 ± 0.03	0	0.43 ± 0.22
OSSF0	NA	(30,50)	0	0.001 ± 0.02	0	0.47 ± 0.24	0	0 ± 0.02	0	0.11 ± 0.09
OSSF0	NA	(0,30)	0	0.007 ± 0.02	1	0.4 ± 0.16	0	0.001 ± 0.02	0	0.02 ± 0.04
OSSF1	off-Z	(100,∞)	0	0.07 ± 0.04	4	1 ± 0.33	0	0.14 ± 0.09	0	0.46 ± 0.2
OSSF1	on-Z	(100,∞)	2	0.6 ± 0.2	2	3.4 ± 0.8	1	0.8 ± 0.41	0	0.6 ± 0.26
OSSF1	off-Z	(50,100)	0	0.21 ± 0.09	5	2.6 ± 0.6	0	0.21 ± 0.11	1	0.7 ± 0.32
OSSF1	on-Z	(50,100)	2	1.3 ± 0.39	10	12 ± 2.5	2	0.6 ± 0.33	1	0.8 ± 0.3
OSSF1	off-Z	(30,50)	1	0.16 ± 0.07	4	2.4 ± 0.5	0	0.06 ± 0.06	0	0.47 ± 0.21
OSSF1	on-Z	(30,50)	3	1.2 ± 0.35	11	14 ± 3.1	0	0.22 ± 0.12	0	0.8 ± 0.31
OSSF1	off-Z	(0,30)	1	0.38 ± 0.18	11	5.7 ± 1.7	0	0.05 ± 0.04	0	0.5 ± 0.26
OSSF1	on-Z	(0,30)	1	2 ± 0.5	32	30 ± 9.2	1	0.19 ± 0.11	3	1.3 ± 0.42
OSSF2	TwoZ	(100,∞)	0	0.02 ± 0.15	–	–	0	0.21 ± 0.13	–	–
OSSF2	OneZ	(100,∞)	1	0.43 ± 0.15	–	–	0	0.5 ± 0.29	–	–
OSSF2	off-Z	(100,∞)	0	0.06 ± 0.03	–	–	0	0.09 ± 0.07	–	–
OSSF2	TwoZ	(50,100)	3	2.8 ± 2.1	–	–	0	0.33 ± 0.11	–	–
OSSF2	OneZ	(50,100)	1	2 ± 0.7	–	–	1	0.5 ± 0.28	–	–
OSSF2	off-Z	(50,100)	2	0.2 ± 0.14	–	–	0	0.12 ± 0.1	–	–
OSSF2	TwoZ	(30,50)	19	22 ± 9	–	–	2	0.7 ± 0.24	–	–
OSSF2	OneZ	(30,50)	6	6.5 ± 2.4	–	–	0	0.32 ± 0.12	–	–
OSSF2	off-Z	(30,50)	3	1.4 ± 0.6	–	–	1	0.15 ± 0.08	–	–
OSSF2	TwoZ	(0,30)	118	109 ± 28	–	–	3	2 ± 0.5	–	–
OSSF2	OneZ	(0,30)	24	29 ± 7.6	–	–	1	0.6 ± 0.17	–	–
OSSF2	off-Z	(0,30)	5	7.8 ± 2.3	–	–	0	0.18 ± 0.06	–	–

Table 7: Observed yields for four lepton events from 19.5 fb^{-1} data recorded in 2012. The channels are broken down by the number of and mass of any opposite-sign, same-flavor pairs (whether on or off Z), whether there are any b-jets present and the E_T^{miss}. Expected yields are the sum of simulation and data-driven estimates of backgrounds in each channel. The channels are exclusive.

3 Lepton Results										
Selection		E_T^{miss}	N(τ)=0, NbJet=0		N(τ)=1, NbJet=0		N(τ)=0, NbJet≥1		N(τ)=1, NbJet≥1	
			obs	expect	obs	expect	obs	expect	obs	expect
OSSF0(SS)		(200,∞)	1	1.3 ± 0.6	2	1.4 ± 0.5	0	0.7 ± 0.36	0	0.7 ± 0.5
OSSF0(SS)		(150,200)	2	2.1 ± 0.9	0	3 ± 1.1	1	2.1 ± 1	0	1.5 ± 0.6
OSSF0(SS)		(100,150)	9	10 ± 4.9	4	9.9 ± 3	12	12 ± 5.9	4	6.3 ± 2.8
OSSF0(SS)		(50,100)	34	37 ± 15	54	66 ± 14	32	32 ± 15	24	22 ± 10
OSSF0(SS)		(0,50)	47	46 ± 11	196	221 ± 51	28	24 ± 11	21	31 ± 9.6
OSSF0		(200,∞)	–	–	5	4.8 ± 2.4	–	–	6	5.9 ± 3.1
OSSF0		(150,200)	–	–	12	18 ± 9.1	–	–	21	20 ± 10
OSSF0		(100,150)	–	–	94	96 ± 47	–	–	91	121 ± 61
OSSF0		(50,100)	–	–	351	329 ± 173	–	–	300	322 ± 163
OSSF0		(0to50)	–	–	682	767 ± 207	–	–	230	232 ± 118
OSSF1	below-Z	(200,∞)	2	2.5 ± 0.9	4	2.1 ± 1	1	1.9 ± 0.7	2	2.4 ± 1.2
OSSF1	on-Z	(200,∞)	17	19 ± 6.3	4	5.6 ± 1.9	1	2.4 ± 0.8	3	2.1 ± 0.9
OSSF1	below-Z	(150,200)	7	4.4 ± 1.7	11	9.3 ± 4.6	3	4.7 ± 2.1	7	11 ± 5.9
OSSF1	on-Z	(150,200)	38	32 ± 8.5	10	11 ± 3.6	4	5.4 ± 1.7	2	5.7 ± 2.7
OSSF1	below-Z	(100,150)	21	26 ± 9.9	45	56 ± 27	20	23 ± 11	56	66 ± 33
OSSF1	on-Z	(100,150)	134	129 ± 29	43	51 ± 16	20	18 ± 6	24	28 ± 14
OSSF1	below-Z	(50,100)	157	129 ± 30	383	380 ± 104	58	60 ± 28	166	173 ± 87
OSSF1	on-Z	(50,100)	862	732 ± 141	1363	1227 ± 323	80	62 ± 17	117	101 ± 48
OSSF1	below-Z	(0,50)	543	559 ± 93	10186	9171 ± 2714	40	52 ± 14	257	256 ± 79
OSSF1	on-Z	(0,50)	4041	4061 ± 691	51361	51369 ± 15340	181	181 ± 28	1003	1012 ± 286

Table 8: Observed yields for three lepton events from 19.5 fb^{-1} data recorded in 2012. The channels are broken down by the number of and mass of any opposite-sign, same-flavor pairs (whether on or off Z), whether there are any b-jets present and the E_T^{miss}. Expected yields are the sum of simulation and data-driven estimates of backgrounds in each channel. The channels are exclusive.

2 Lepton and 2 Photon Results				
Selection		E_T^{miss}	obs	expect
OSSF1	off-Z	(50,∞)	0	0.19±0.25
OSSF1	on-Z	(50,∞)	0	0.1±0.17
OSSF1	off-Z	(30,50)	1	0.17±0.25
OSSF1	on-Z	(30,50)	1	0.33±0.28
OSSF1	off-Z	(0,30)	1	1.2±0.74
OSSF1	on-Z	(0,30)	0	1.01±0.55
OSSF0	NA	(0,∞)	0	0±0.17

Table 9: Observed yields for two lepton and two photon events from 19.5 fb^{-1} data recorded in 2012. The channels are broken down the number of and mass of any opposite-sign, same-flavor pairs (whether on or off Z), and the E_T^{miss}. Only channels where invariant mass of photons lies in the higgs mass window (120-130 GeV) are considered. Expected yields are data-driven estimates of backgrounds in each channel. The channels are exclusive.

1 Lepton and 2 Photon Results		
E_T^{miss}	obs	expect
(50,∞)	9	14.3±7.15
(30,50)	31	22.1±11.05
(0,30)	74	79.1±39.55

Table 10: Observed yields for one lepton and diphoton events from 19.5 fb^{-1} data recorded in 2012. The channels are broken down in bins of E_T^{miss}. There are no hadronic taus in these channels. Only channels where the invariant mass of photons lies in the higgs mass window (120-130 GeV) are considered. Expected yields are data-driven estimates of backgrounds in each channel. The channels are exclusive.

Multi-lepton and Photons: Results

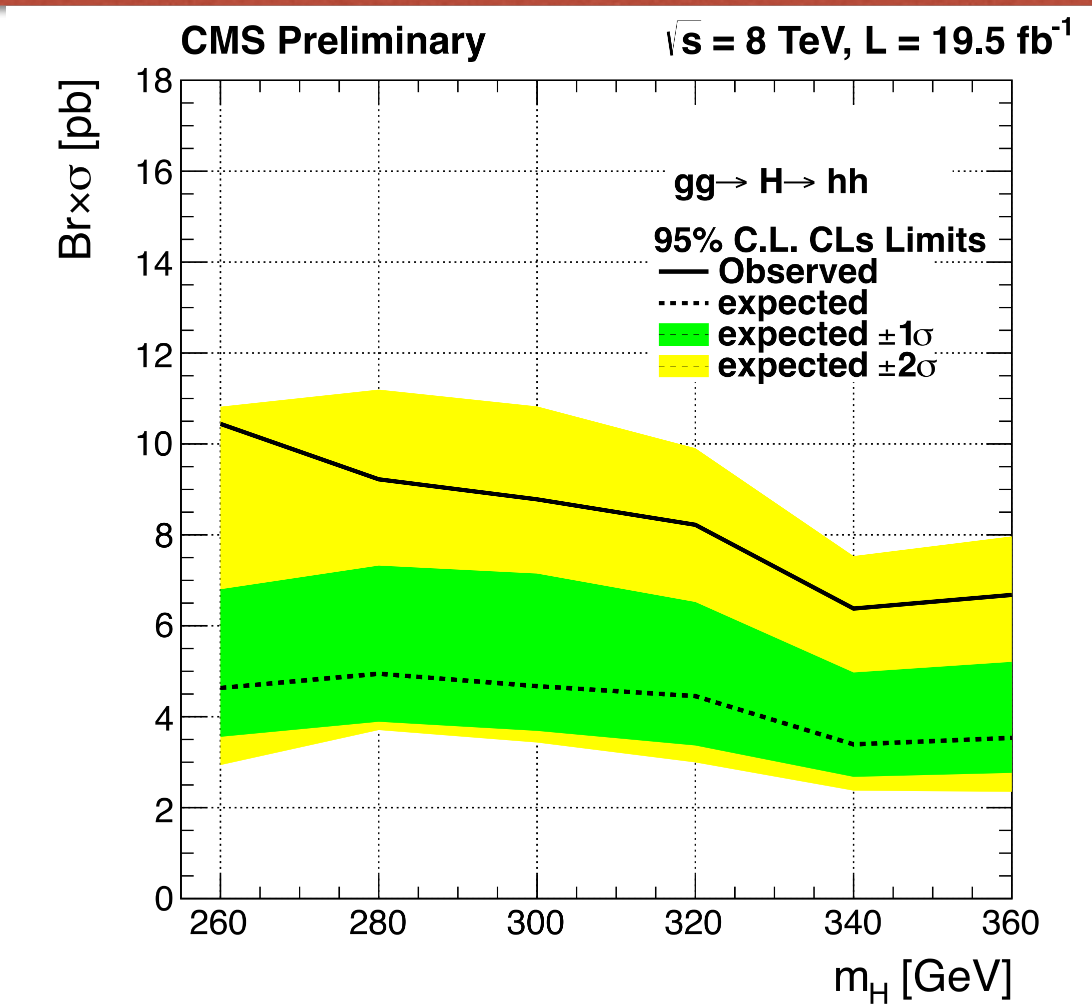

Figure 6: Observed and expected limits with 1- and 2-σ bands for $H \to hh$ in terms of σ * Br. These limits are based only on multilepton channels. Brs for h are assumed to have SM values. No contribution from gg→A→Zh is considered in this limit.

$$\Delta L = -\sum_{i=1,2} (y_i^u Q\tilde{\Phi}_i\bar{u} + y_i^d Q\Phi_i\bar{d} + y_i^e L\Phi_i\bar{e} + h.c.)$$

- Type 1, in which $y_1^{u,d,e} = 0$; all fermions couple to one doublet.
- Type 2, in which $y_1^u = y_2^d = y_2^e = 0$; the up-type quarks couple to one doublet and the down-type quarks and leptons couple to the other.
- Type 3, in which $y_1^u = y_1^d = y_2^e = 0$; quarks couple to one doublet and leptons to the other.
- Type 4, in which $y_1^u = y_1^e = y_2^d = 0$; up-type quarks and leptons couple to one doublet and down-type quarks couple to the other.

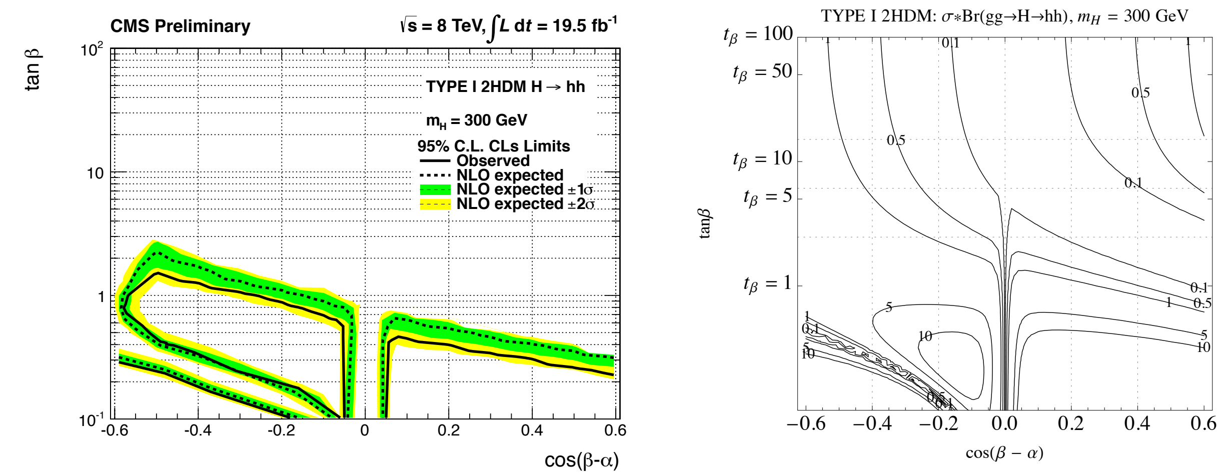

Figure 11: Left: Observed and expected limits on Heavy higgs of mass 300 GeV in Type I 2HDM. The parameters α and β determine the cross section for H production, the Br$(H \to hh)$ and the Br$(h \to WW, ZZ, \tau\tau, \gamma\gamma)$. Right: The σ * Br(H→hh) contours for TYPE I 2HDM. This figure is similar to one from theory paper by Nathaniel Craig et al. [4], the only difference is plotting of $\tan\beta$, instead of β, on the vertical axis. The regions below the observed limit lines and within the loop by marked by observed limit are excluded.

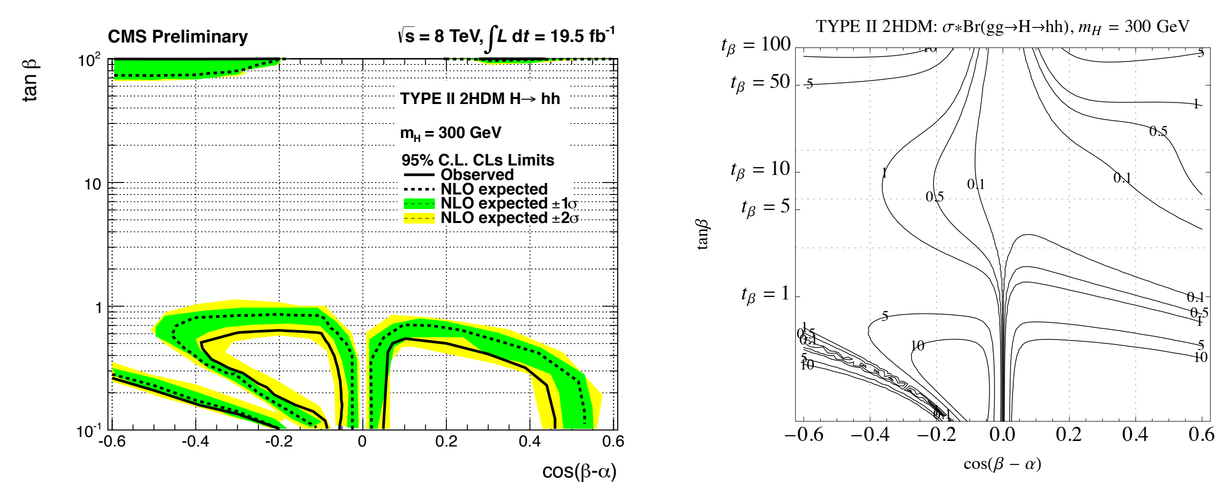

Figure 12: Left: Observed and expected limits on Heavy higgs of mass 300 GeV in Type II 2HDMs. The parameters α and β determine the cross section for H production, the Br$(H \to hh)$ and the Br$(h \to WW, ZZ, \tau\tau, \gamma\gamma)$. Right: The σ * Br(H→hh) contours for TYPE II 2HDM. This figure is similar to one from theory paper by Nathaniel Craig et al. [4], the only difference is plotting of $\tan\beta$, instead of β, on the vertical axis. The regions below the observed limit lines and within the loop by marked by observed limit are excluded.

H(bb̄)H(γγ): Signal Spectra

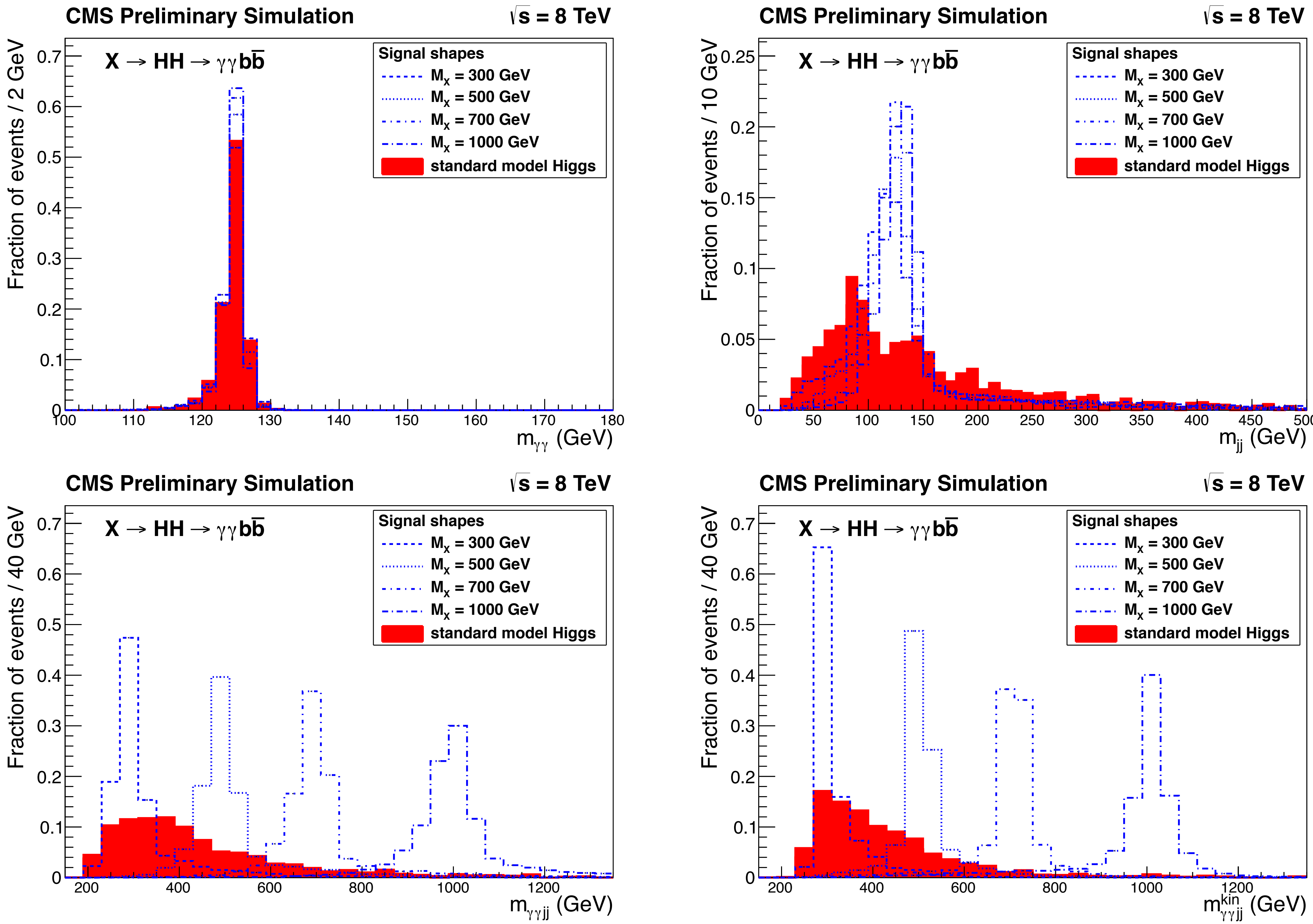

Figure 1: Simulated mass spectra for the signal and the sum of all production mechanisms of the standard model Higgs boson, after basic selections on photons and requesting at least one loose b–tagged jet. The two top plots show the $m_{\gamma\gamma}$ (left) and m_{jj} (right) spectra, while the bottom plots show the $m_{\gamma\gamma jj}$ spectrum before the kinematic fit (left) and after the kinematic fit (right). All spectra are normalized to unity.

H(b$\bar{b}$)H(γγ): Background Fits

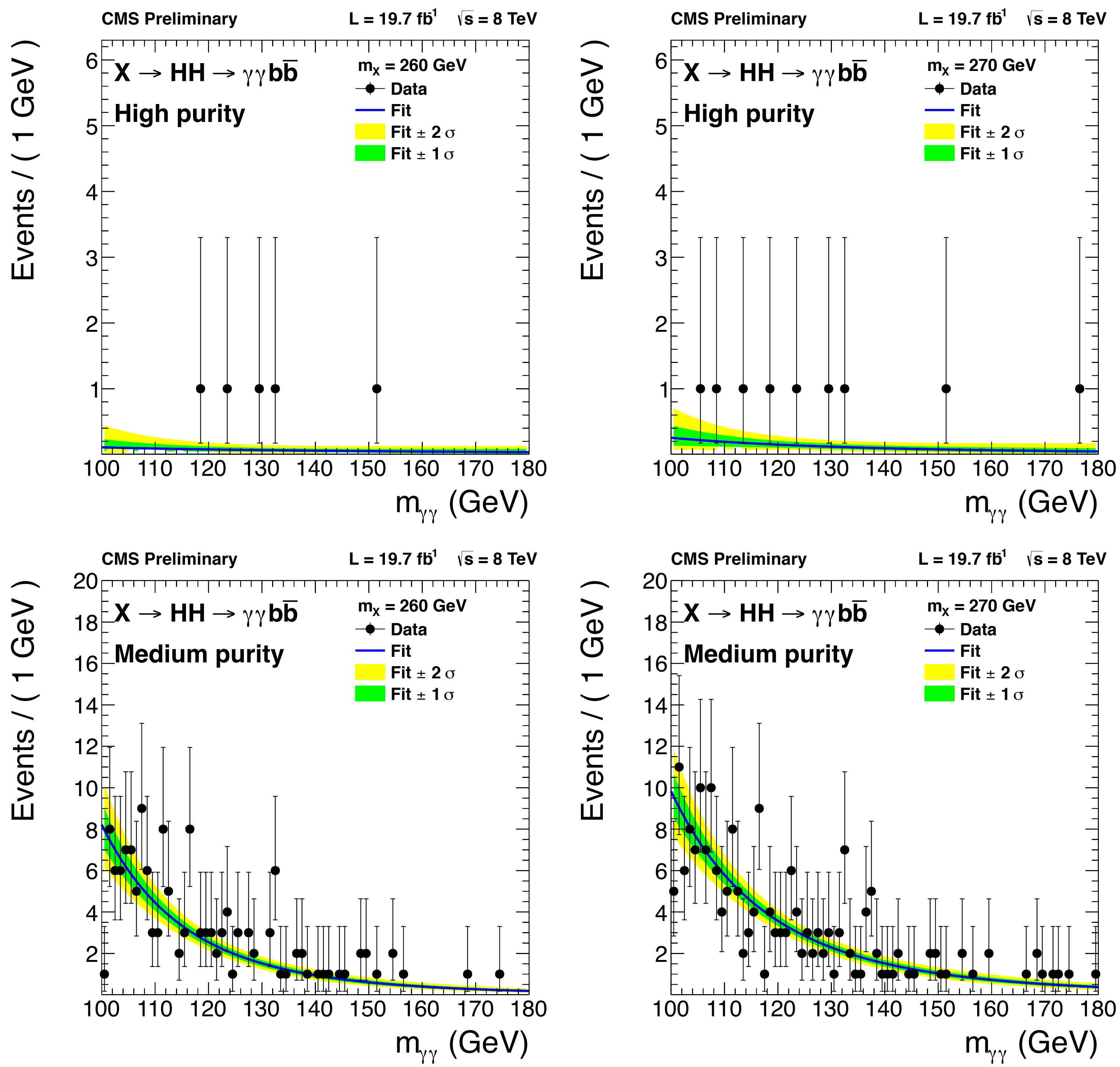

Figure 3: Non-resonant background fits in $m_{\gamma\gamma}$ for the high-purity (top) and medium-purity (bottom) categories for two heavy resonance mass hypotheses - 260 GeV (left) and 270 GeV (right).

$X \to HH \to H(b\bar{b})H(\gamma\gamma)$

Low Mass Regime

Simulated signal shape in $m_{\gamma\gamma}$ for the medium purity category

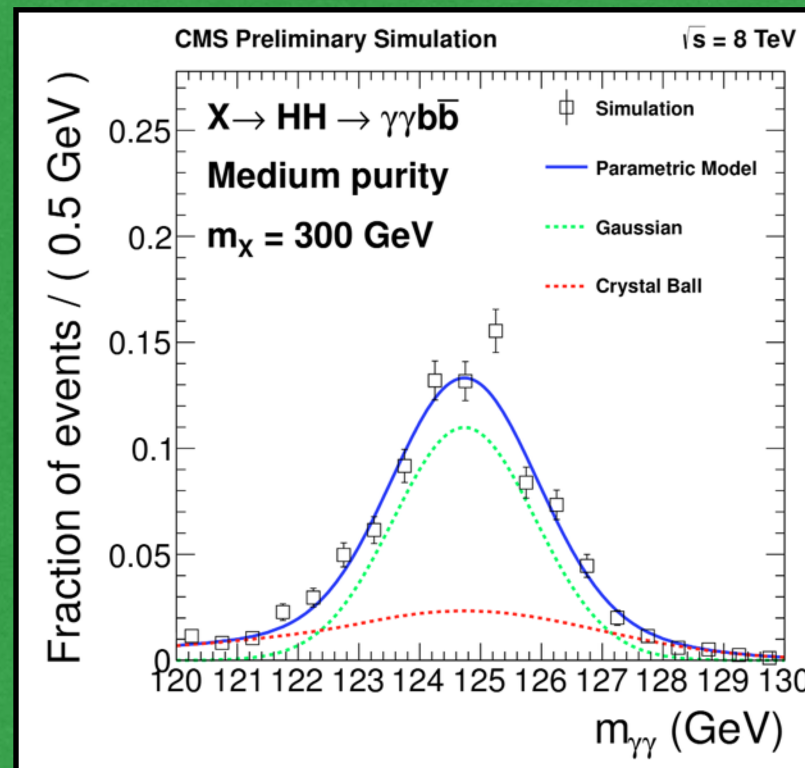

Events in $m_{\gamma\gamma}$ spectrum in medium purity for signal hypothesis of 300 GeV (sliding photon p_T cuts) Fitted to power-law

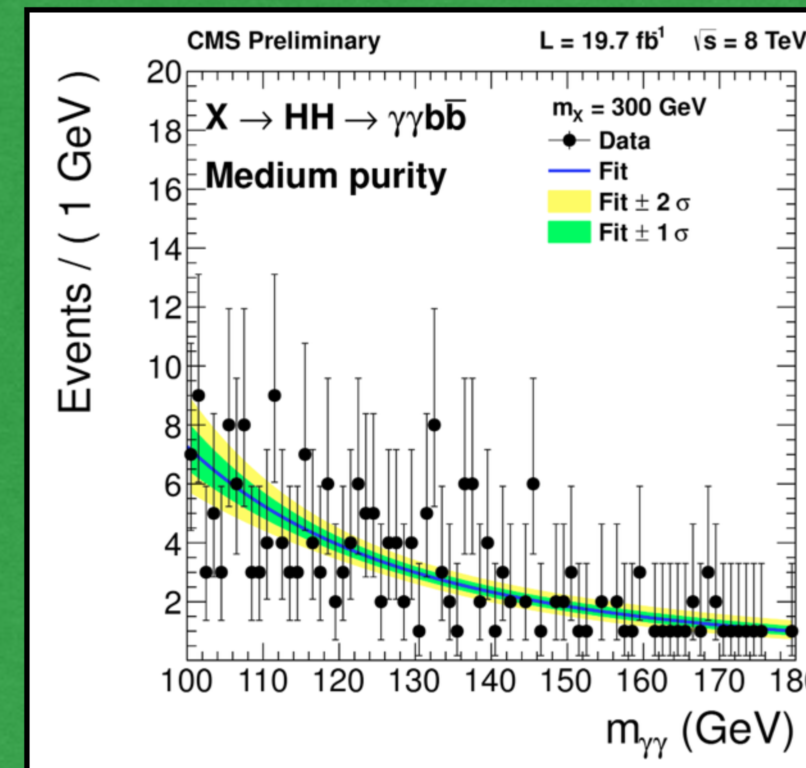

High Mass Regime

Simulated signal shape in $m_{\gamma\gamma jj}^{kinFit}$ for the medium purity category

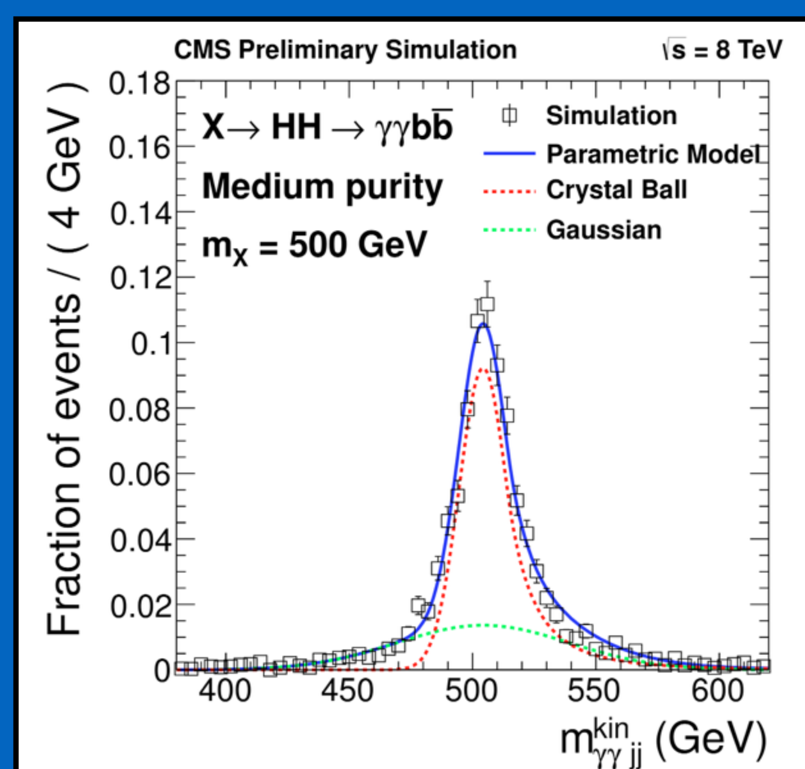

Events in $m_{\gamma\gamma jj}^{kinFit}$ spectrum for signal hypothesis of 500 GeV

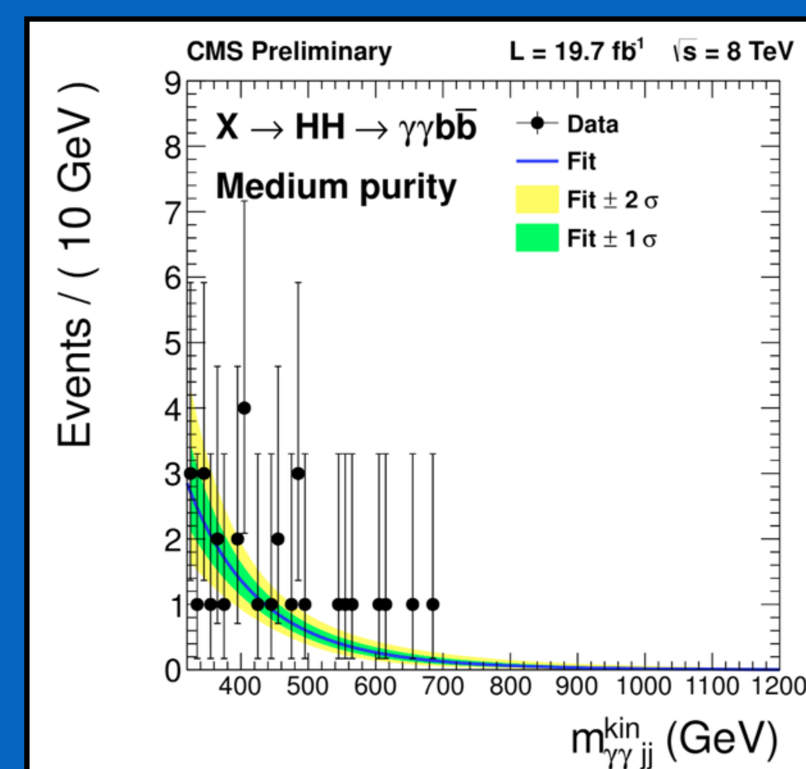

Bias Study

Several “true” background shapes tried. **Negligible bias** on signal strength.

H(b$\bar{b}$)H(γγ): Background Fits

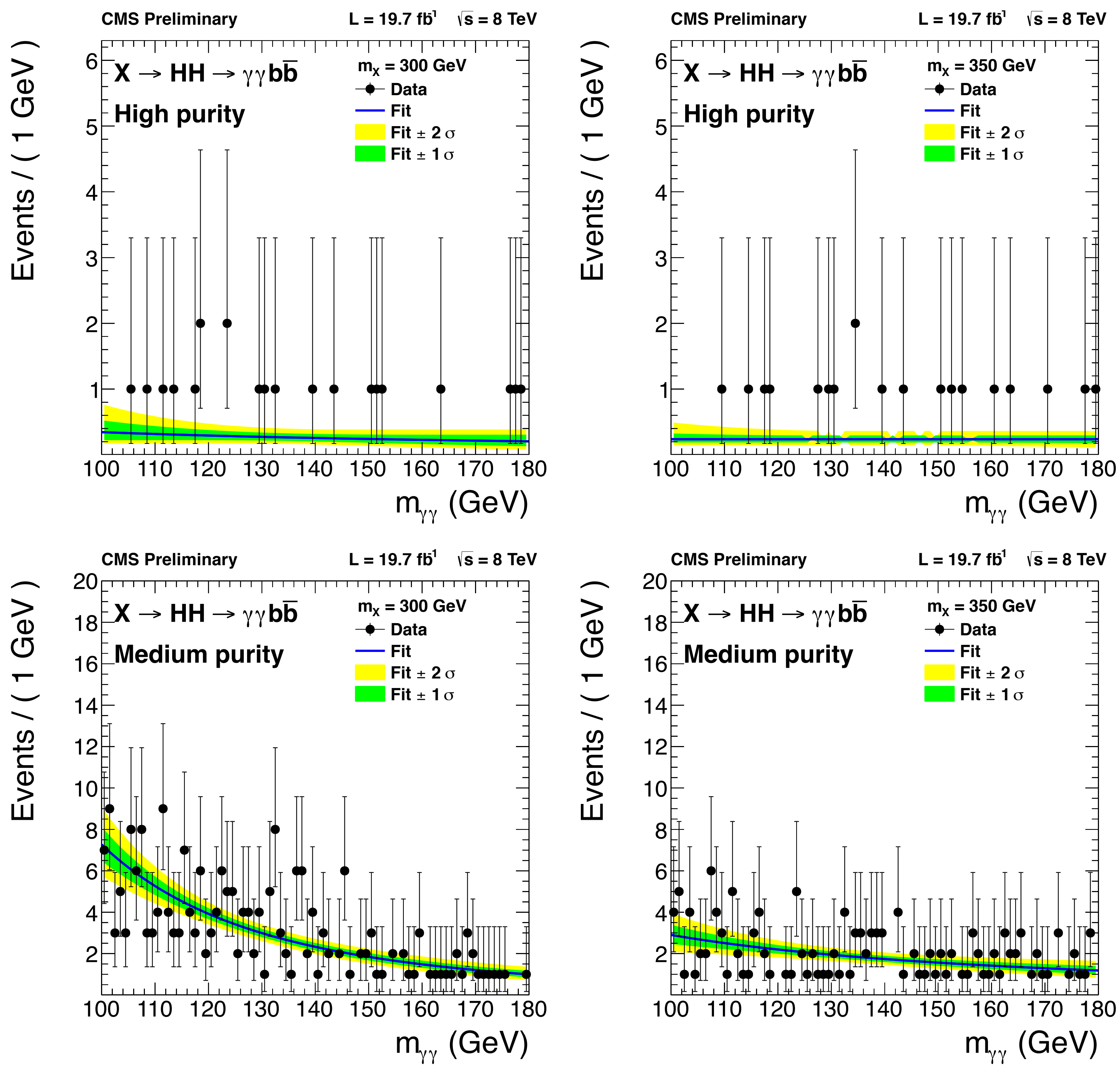

Figure 4: Events in $m_{\gamma\gamma}$ spectrum in high-purity (top) and medium-purity (bottom) categories for two heavy resonance mass hypotheses - 300 GeV (left) and 350 GeV (right). The non-resonant component of the background is shown (black line) with 1 and 2σ bands on the background estimation.

H(b$\bar{b}$)H(γγ): Background Fits

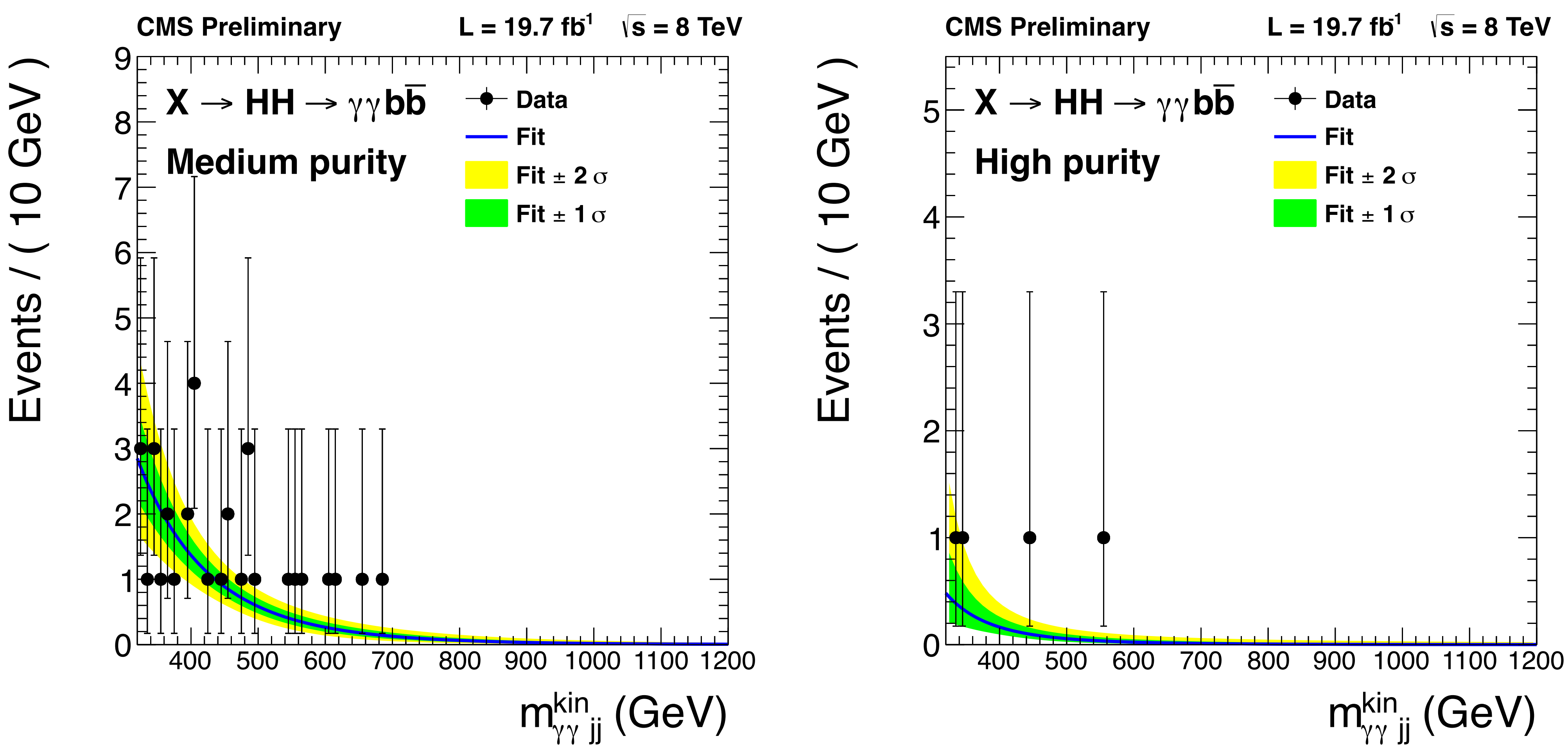

Figure 6: Events in $m_{\gamma\gamma jj}$ spectrum in medium-purity (left) and high-purity (right) categories. The non-resonant component of the background is shown (black line) with 1 and 2σ bands on the background estimation.

$H(b\bar{b})H(\gamma\gamma)$: Systematics

Common normalization uncertainties	
Luminosity	2.6%
Diphoton trigger acceptance	1.0%
Low mass analysis: fit to $m_{\gamma\gamma}$	
Normalization uncertainties	
Photons selection acceptance	1.0%
"b-tag" eff. uncertainty 2 btag cat	4.6%
"b-tag" eff. uncertainty 1 btag cat	-1.2%
m_{jj} and $p_{T,j}$ cut acceptance (JES & JER)	1.5%
$m_{\gamma\gamma jj}$ cut acceptance (PES $\oplus$ JES & PER $\oplus$ JER)	2%
Shape uncertainties	
Parametric scale shift (PES$\oplus$M(H) uncertainty)	$\frac{\Delta m_{\gamma\gamma}}{m_{\gamma\gamma}} = 0.45 \oplus 0.35\%$
Parametric resolution shift (RES)	$\frac{\Delta\sigma}{m_{\gamma\gamma}} = 0.25\%$ $\frac{\Delta\sigma}{\sigma_{\gamma\gamma}} = 22\%$
High mass analysis: fit to $m_{\gamma\gamma jj}^{\mathrm{kin}}$	
Normalization uncertainties	
Photons selection acceptance	1.0%
"b-tag" eff. uncertainty 2 btag cat	5.3%
"b-tag" eff. uncertainty 1 btag cat	-1.8%
m_{jj} and $p_{T,j}$ cut acceptance (JES & JER)	1.5%
$m_{\gamma\gamma}$ cut acceptance (PES & PER)	0.5%
Extra High pt norm. uncertainty	5.0%
Shape uncertainties	
Parametric abs. shift (PES $\oplus$ JES)	$\frac{\Delta m_{\gamma\gamma jj}}{m_{\gamma\gamma jj}} = 0.45 \oplus (0.8 \oplus 1.0) = 1.4\%$
Parametric shift (PER $\oplus$ JER)	$\frac{\Delta\sigma}{\sigma_{\gamma\gamma jj}} = 10\%$

Table 4: Systematic uncertainties by fit strategy.

$H(b\bar{b})H(\gamma\gamma)$: Results

m_X	Observed limit (fb)	Expected limit (fb)	Observed limit (fb)	Expected limit (fb)
			High-purity category only	
260	3.14	2.12	3.54	2.41
270	2.70	2.40	3.07	2.74
300	3.98	2.73	3.64	3.14
350	1.67	2.23	2.17	2.66
400	1.97	1.66	3.40	2.01

m_X	Observed limit (fb)	Expected limit (fb)
400	2.98	1.87
450	1.76	1.42
500	1.19	0.97
550	1.45	0.80
600	0.98	0.69
650	0.61	0.60
700	0.44	0.54
800	0.31	0.46
900	0.32	0.43
1000	0.33	0.43
1100	0.41	0.48

H($b\bar{b}$)H($b\bar{b}$): Signal and $t\bar{t}$ Background

Event Selection Criteria

- Event contains at least 4 jets with p_T > 40 GeV, $|\eta|$ < 2.5, CMVA ϵ = 70%
- **Low Mass Regime**:
  - HH candidates from the selected jets such that $|m_H - 125 \text{ GeV}| < 35$ GeV
  - At least 2 of these jets with p_T > 90 GeV
- **High Mass Regime**:
  - HH candidates from the selected jets such that jets associated with an H have ΔR < 1.5
  - If m_X > 740 GeV, H p_T > 300 GeV
- In case of multiple HH candidates, we choose the combination that minimizes $|m_{H1} - m_{H2}|$
- m_{HH} must fall within SR

Signal Modeling

- Signal shape from simulation of **RS1 radion** decaying to $b\bar{b}b\bar{b}$ via HH.
- **Negligible natural width** 1 GeV
- Samples
  m_X = 270 GeV to 1100 GeV

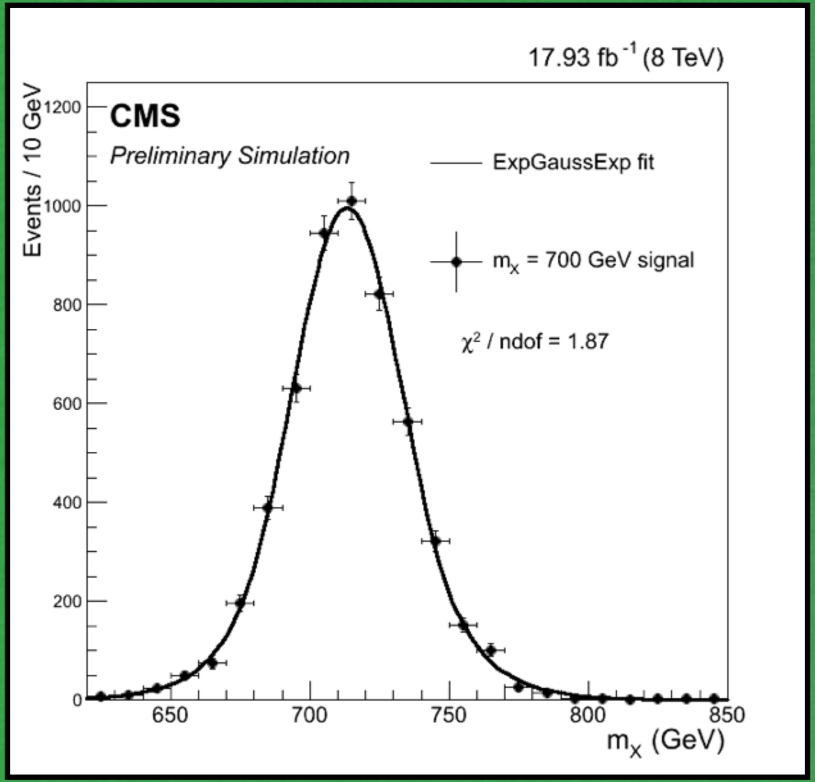

$t\bar{t}$ Modeling

- $t\bar{t}$ contributes **22% (27%)** of background in Low (High) mass regimes
- Modeled from MC.

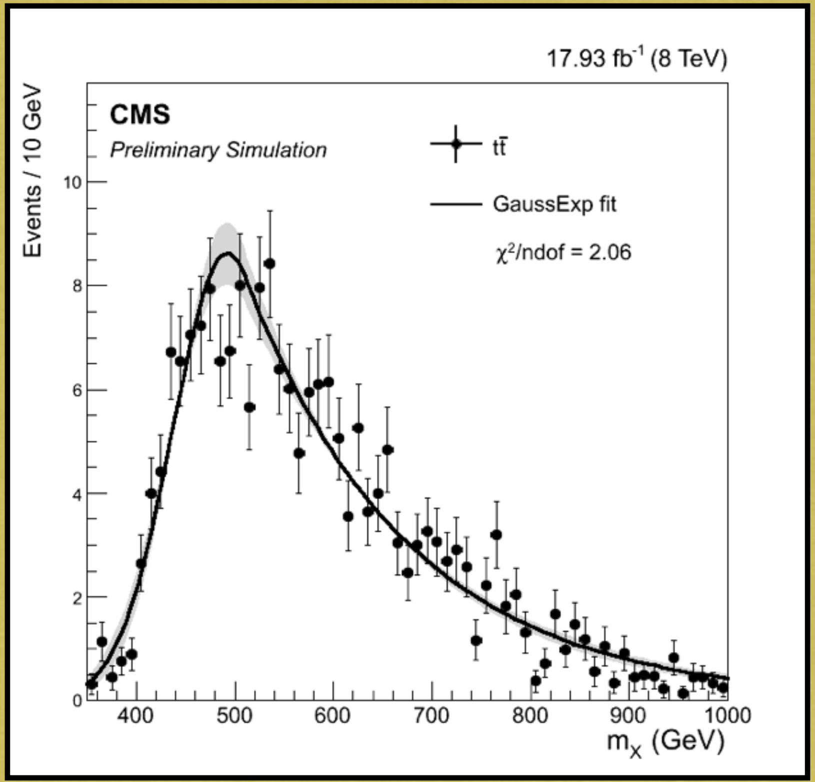

H($b\bar{b}$)H($b\bar{b}$): Combined MVA tagger

The CMVA tagger combines features from different b-taggers:

- Jet Probability for IP
- CSV for combining SV information
- Soft leptons information when available
- Inclusive Vertex Finder to determine Secondary Vertices

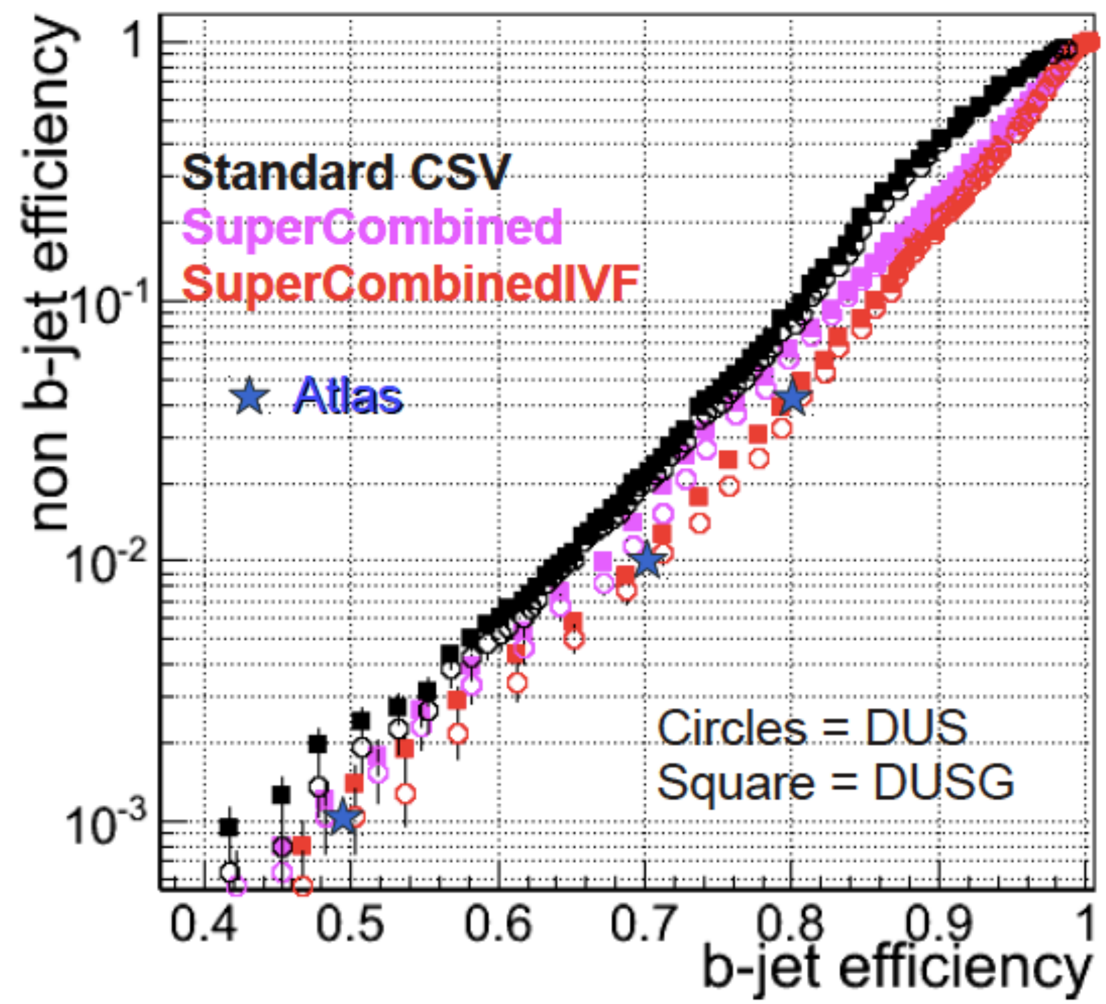

- **2x better fake rejection at 70% efficiency**

- CMVA SF for MC computed as a correction to CSV SF, determined in a $t\bar{t}$ enriched region of data

- ±1σ variations of this scale factors propagates to a 12.7% systematic uncertainty on the signal efficiency

$H(b\bar{b})H(b\bar{b})$: Signal Modeling and Efficiencies

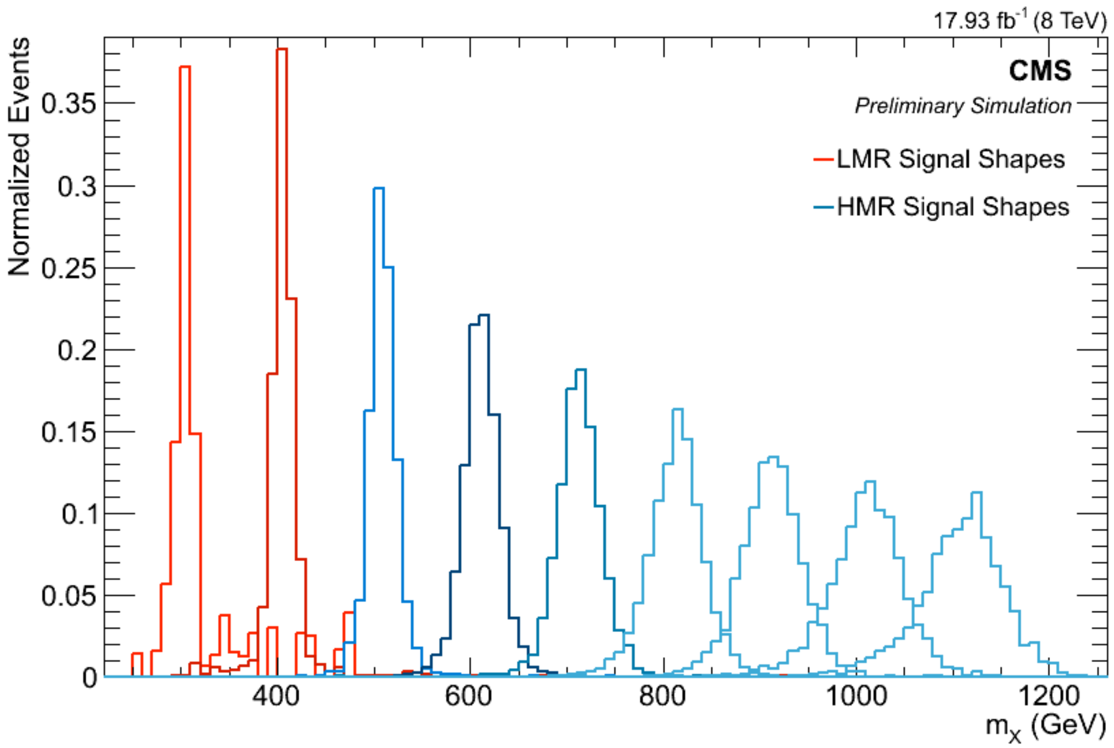

The m_X distribution of signal events after the event selection criteria for each of mass hypothesis. Momenta of b-jets have been corrected by the kinematic constraint to m_H

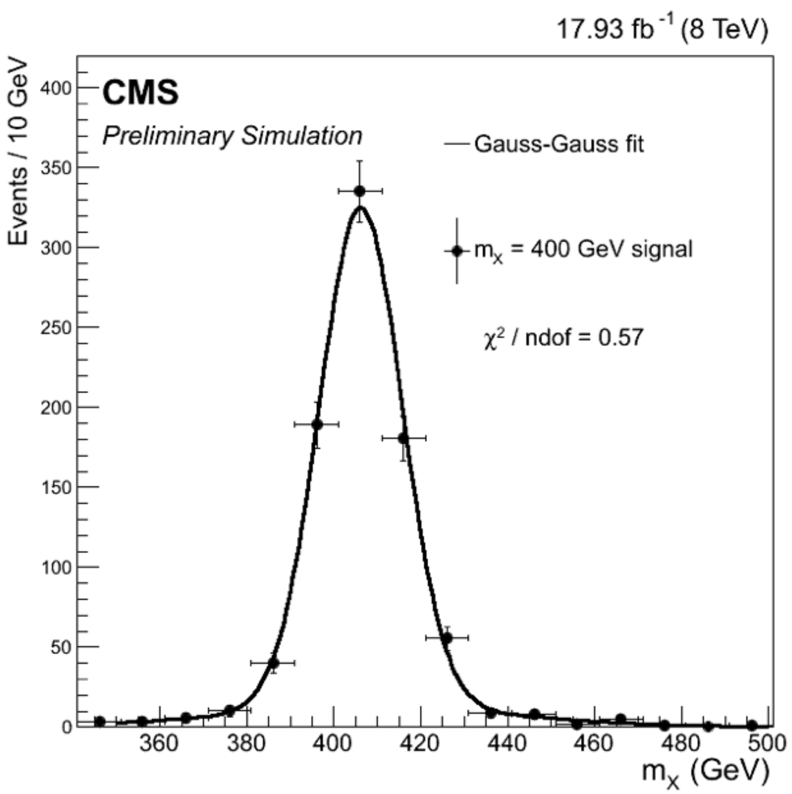

The sum of two Gaussians fitted to the mX= 400 GeV distribution of simulated signal events after the event selection criteria for the Low Mass Regime.

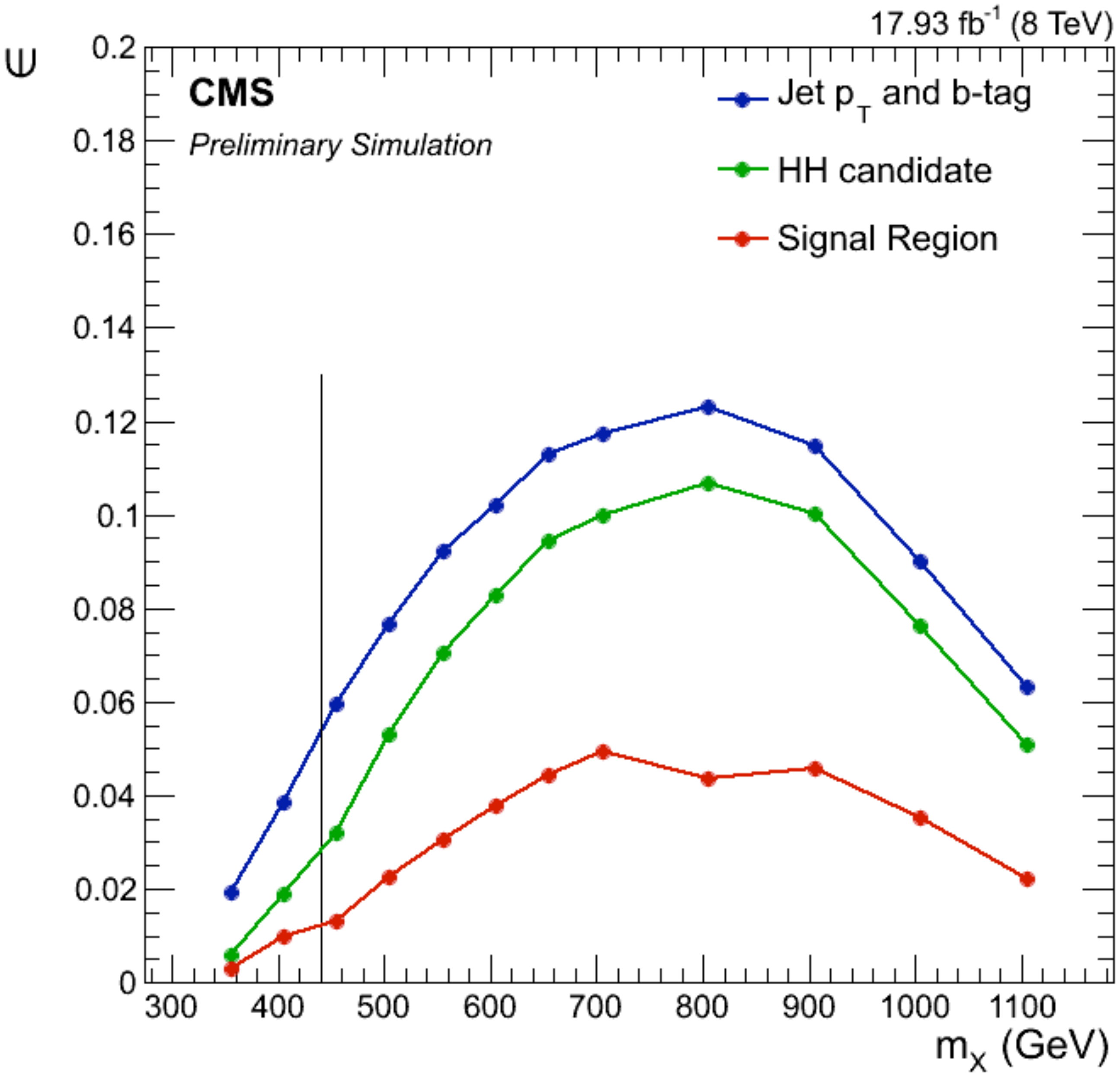

The selection efficiency for X to $H(b\bar{b})H(b\bar{b})$ signal events at different stages of the event selection for each mass hypothesis. The vertical lines represents the transition from the Low Mass Regime and the High Mass Regime as evaluated to optimize the expected significance.

$H(b\bar{b})H(b\bar{b})$: Background Composition

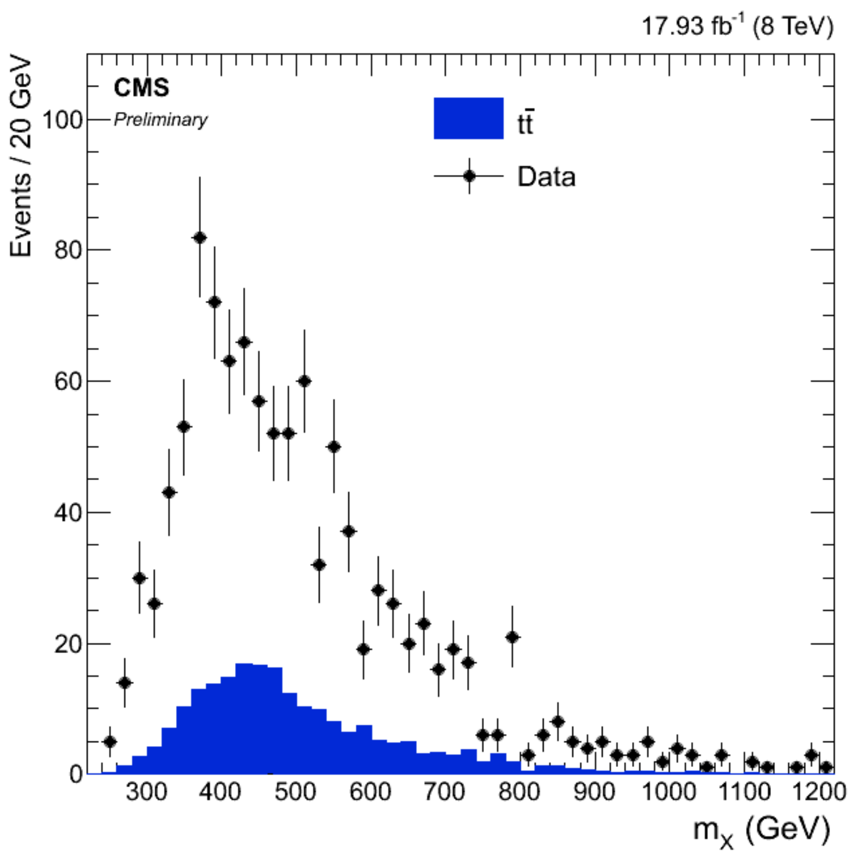

	LMR (%)	MMR & HMR (%)
Z + jets	< 0.1	< 0.04
ZZ	0.003	0.003
ZH	< 0.001	< 0.004
tt	22	27

The contribution of Z+jets, ZZ, ZH and $t\bar{t}$ to the background after all selection criteria. The remainder of the background comes from QCD multi-jet events

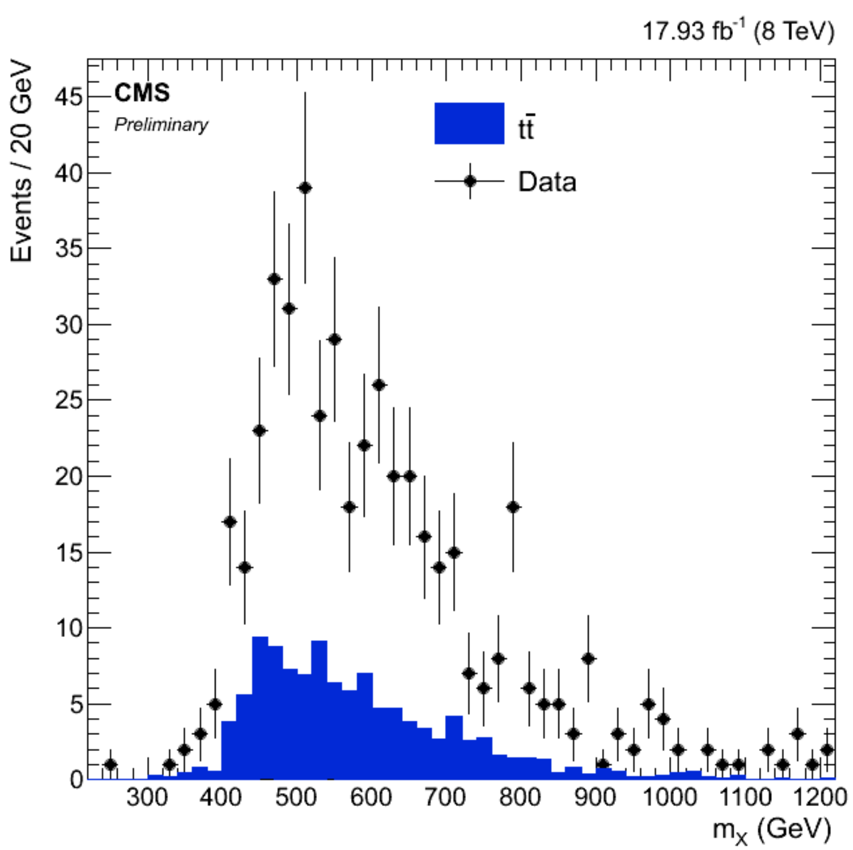

The $t\bar{t}$ composition of the data events in the SR region for the Low Mass Region (top) and the High Mass Region (bottom) as estimated in simulation. All event weights to correct for data/MC differences in pile-up, trigger and b-tagging efficiencies have been applied. Momenta of b-jets have been corrected by the kinematic constraint to m_H.

H(b$\bar{b}$)H(b$\bar{b}$): t$\bar{t}$ Modeling

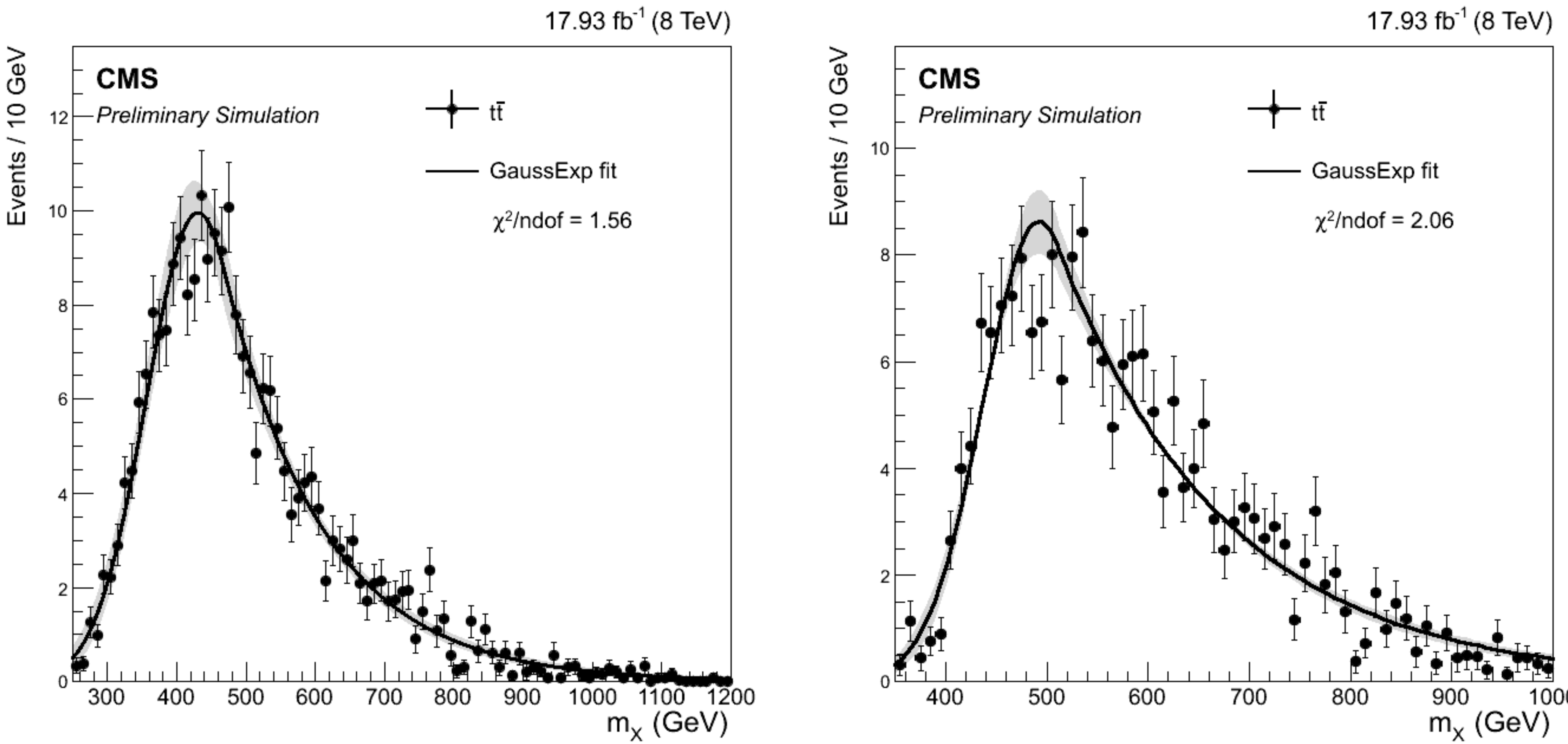

The m_X of simulated ttbar events after the event selection criteria for the Low Mass Region (left) and High Mass Region (right). The distributions are fitted to the GaussExp function

$H(b\bar{b})H(b\bar{b})$: QCD Multi-jet Modeling

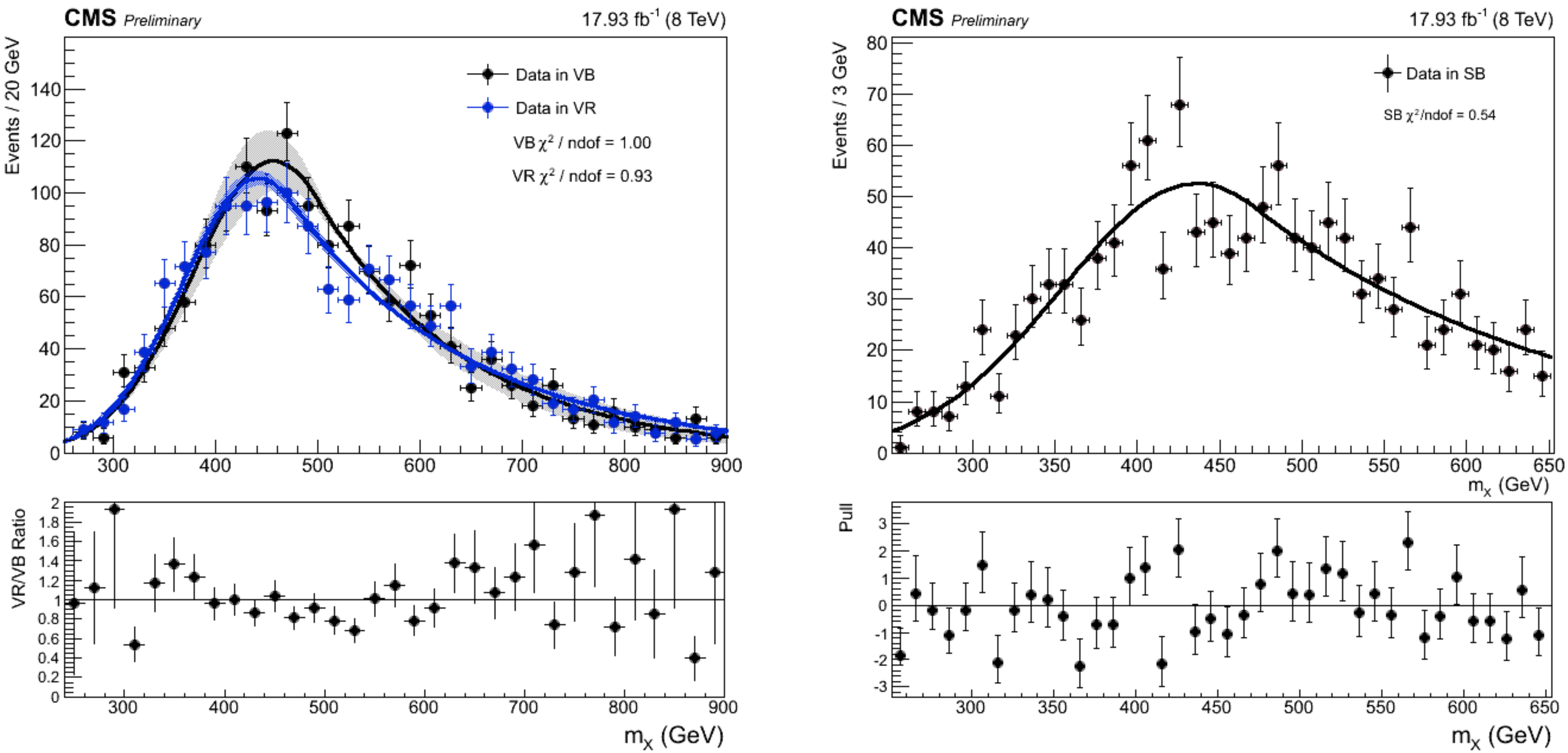

Low Mass Region: The m_X distributions of the QCD multi-jet component of the background in the Validation Region & Sideband (VR & VB) on the left and the Signal Region Sideband (SB) of LMR. The distributions are fitted to the GaussExp function.

H(b$\bar{b}$)H(b$\bar{b}$): QCD Multi-jet Modeling

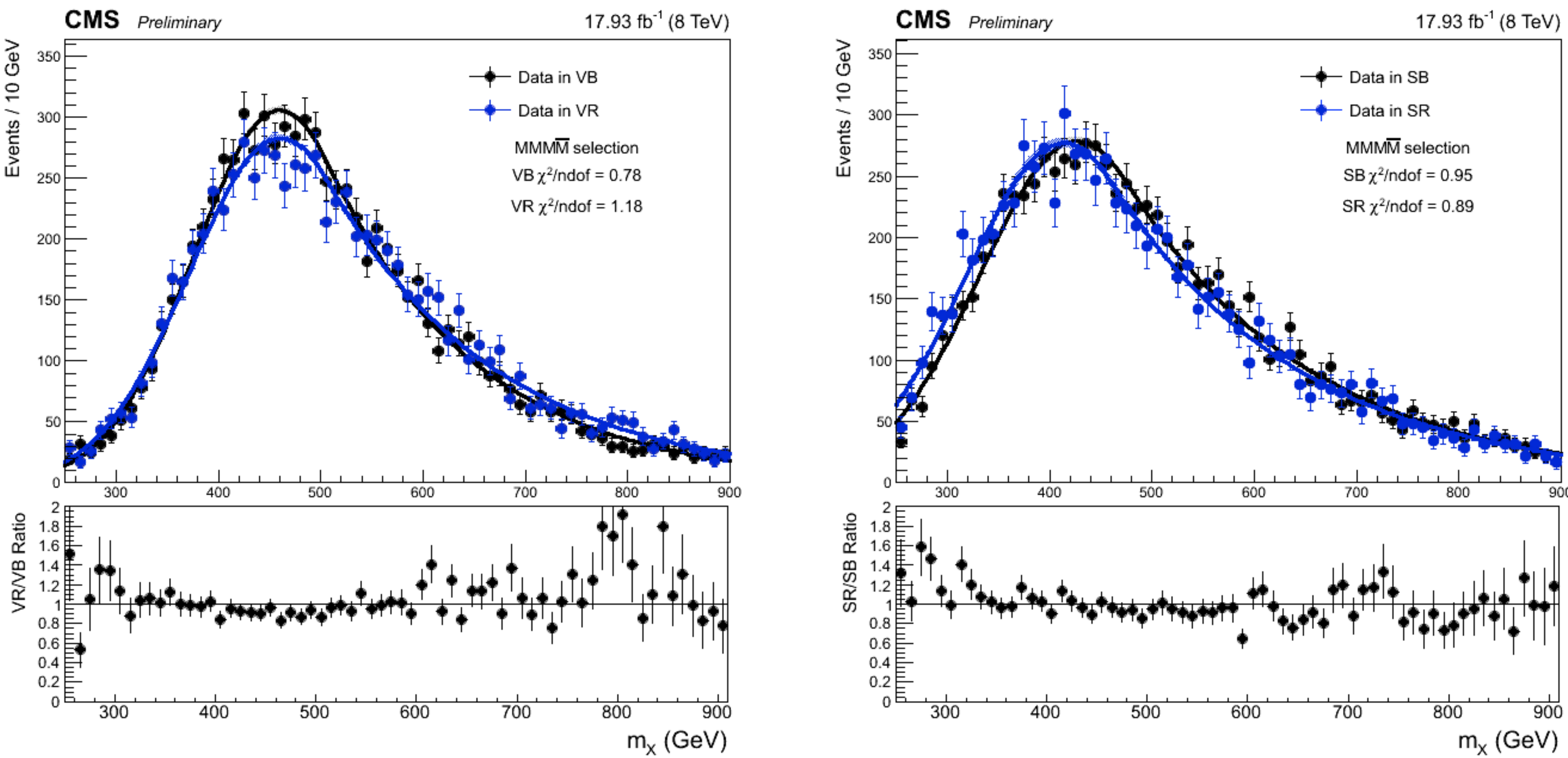

Low Mass Region, anti-btag Control Region: The m_X distributions of the QCD multi-jet component of the background in the Validation Region & Sideband (VR & VB) on the left and the Signal Region Sideband (SB) of LMR. The distributions are fitted to the GaussExp function.

H($b\bar{b}$)H($b\bar{b}$): QCD Multi-jet Modeling

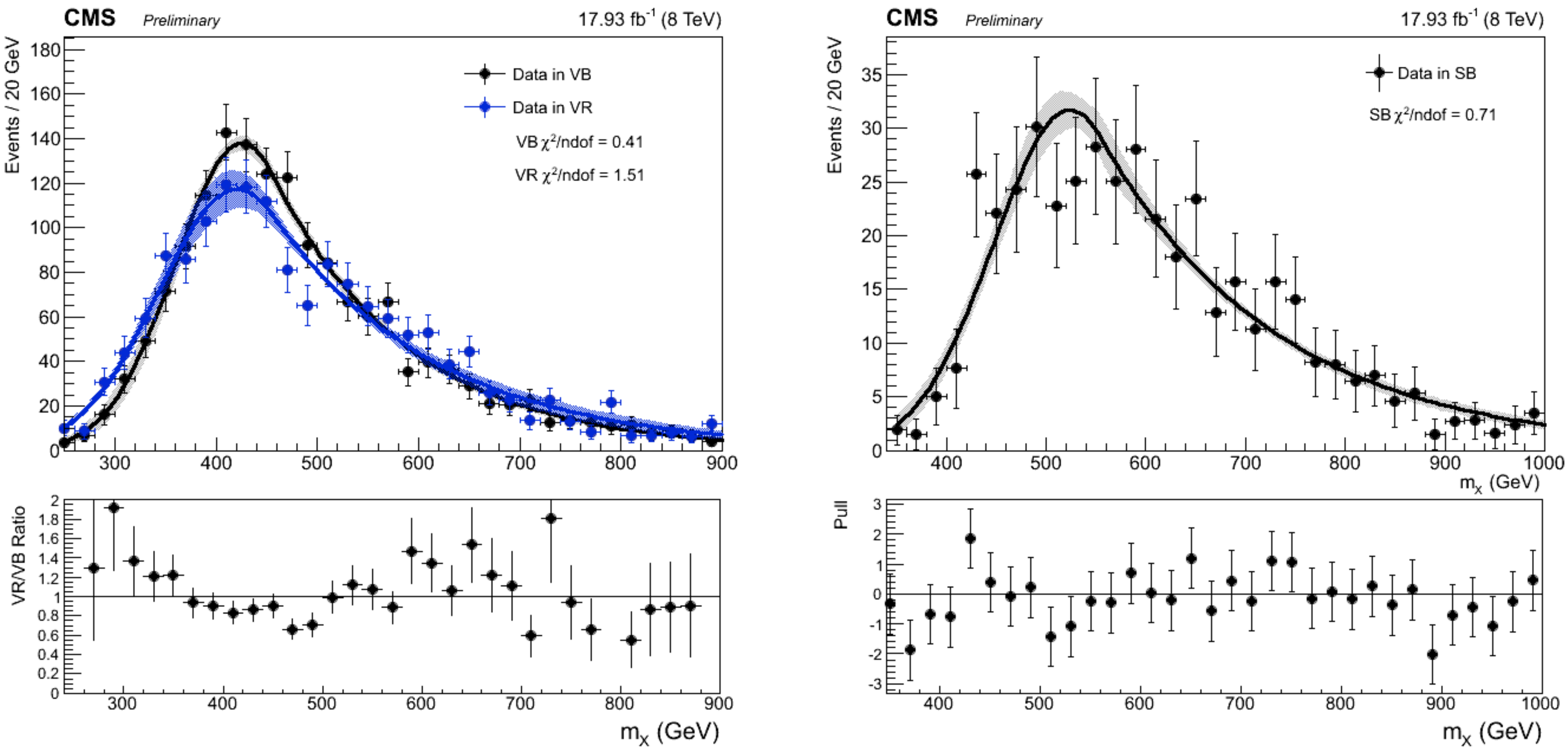

Medium Mass Region: The m_X distributions of the QCD multi-jet component of the background in the Validation Region & Sideband (VR & VB) on the left and the Signal Region Sideband (SB) of LMR. The distributions are fitted to the GaussExp function.

$H(b\bar{b})H(b\bar{b})$: QCD Multi-jet Modeling

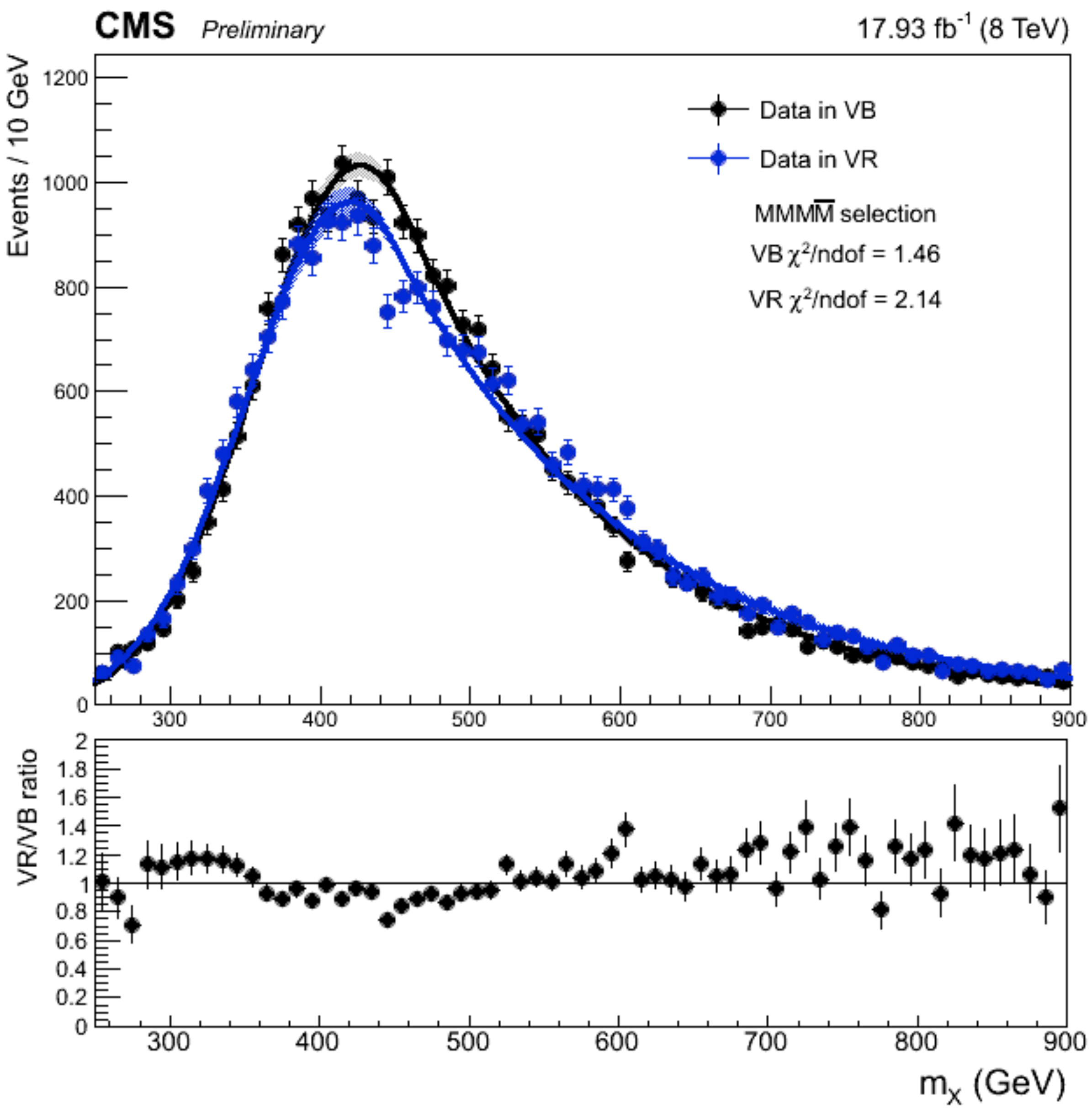

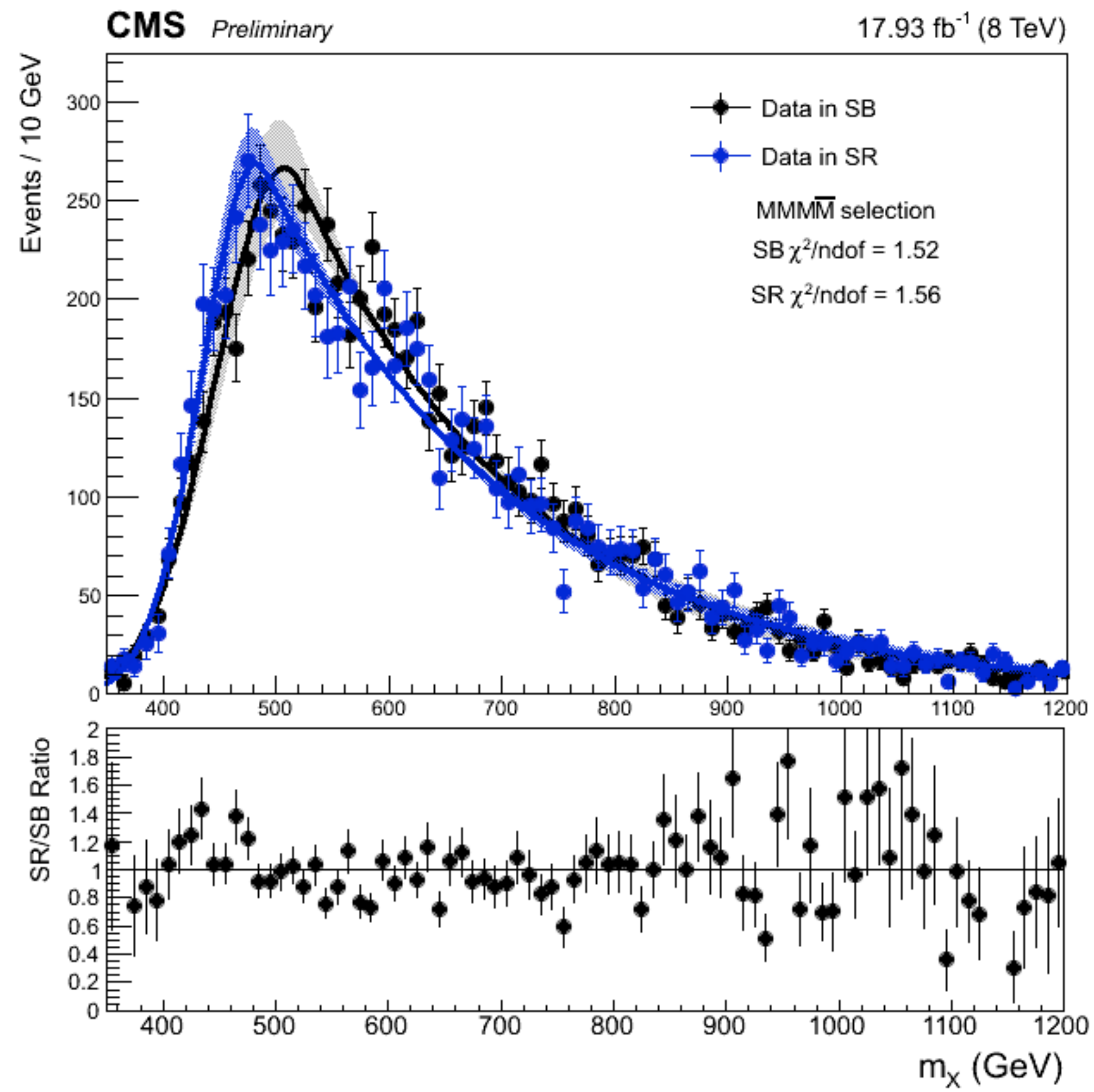

Medium Mass Region, anti-btag Control Region: The m_X distributions of the QCD multi-jet component of the background in the Validation Region & Sideband (VR & VB) on the left and the Signal Region Sideband (SB) of LMR. The distributions are fitted to the GaussExp function.

H(b$\bar{b}$)H(b$\bar{b}$): QCD Multi-jet Modeling

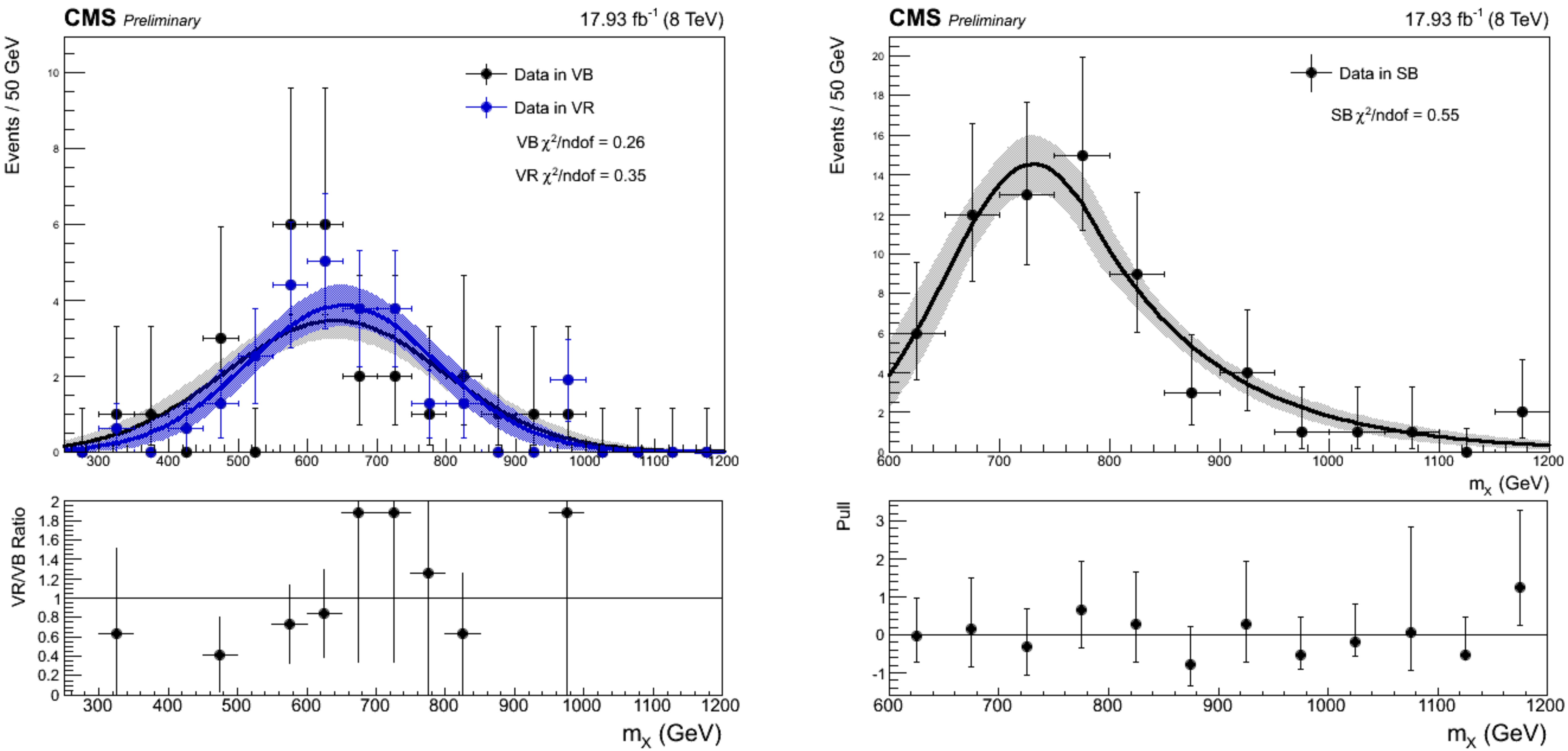

High Mass Region: The m_X distributions of the QCD multi-jet component of the background in the Validation Region & Sideband (VR & VB) on the left and the Signal Region Sideband (SB) of LMR. The distributions are fitted to the GaussExp function.

H(bb̄)H(bb̄): QCD Multi-jet Modeling

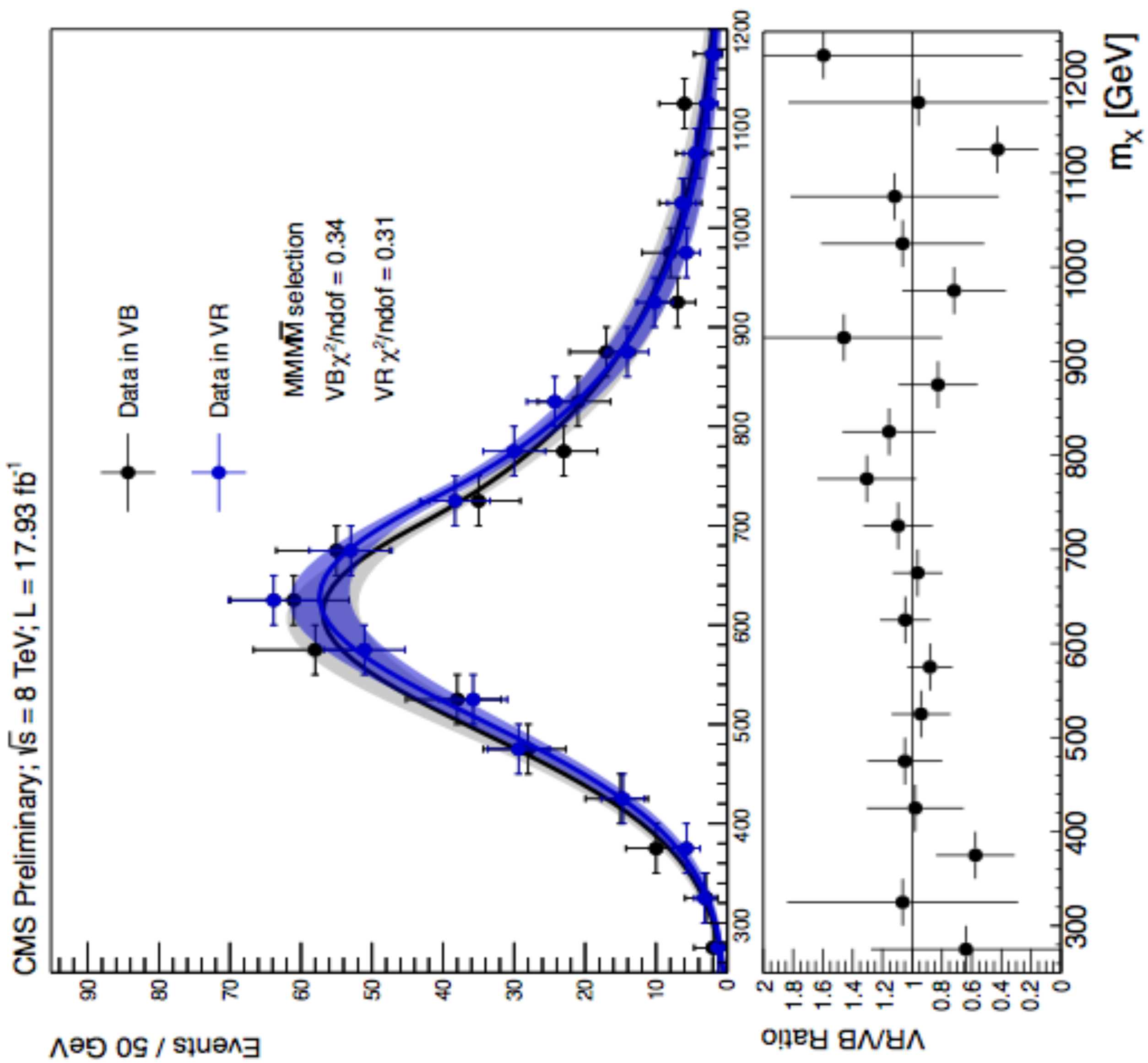

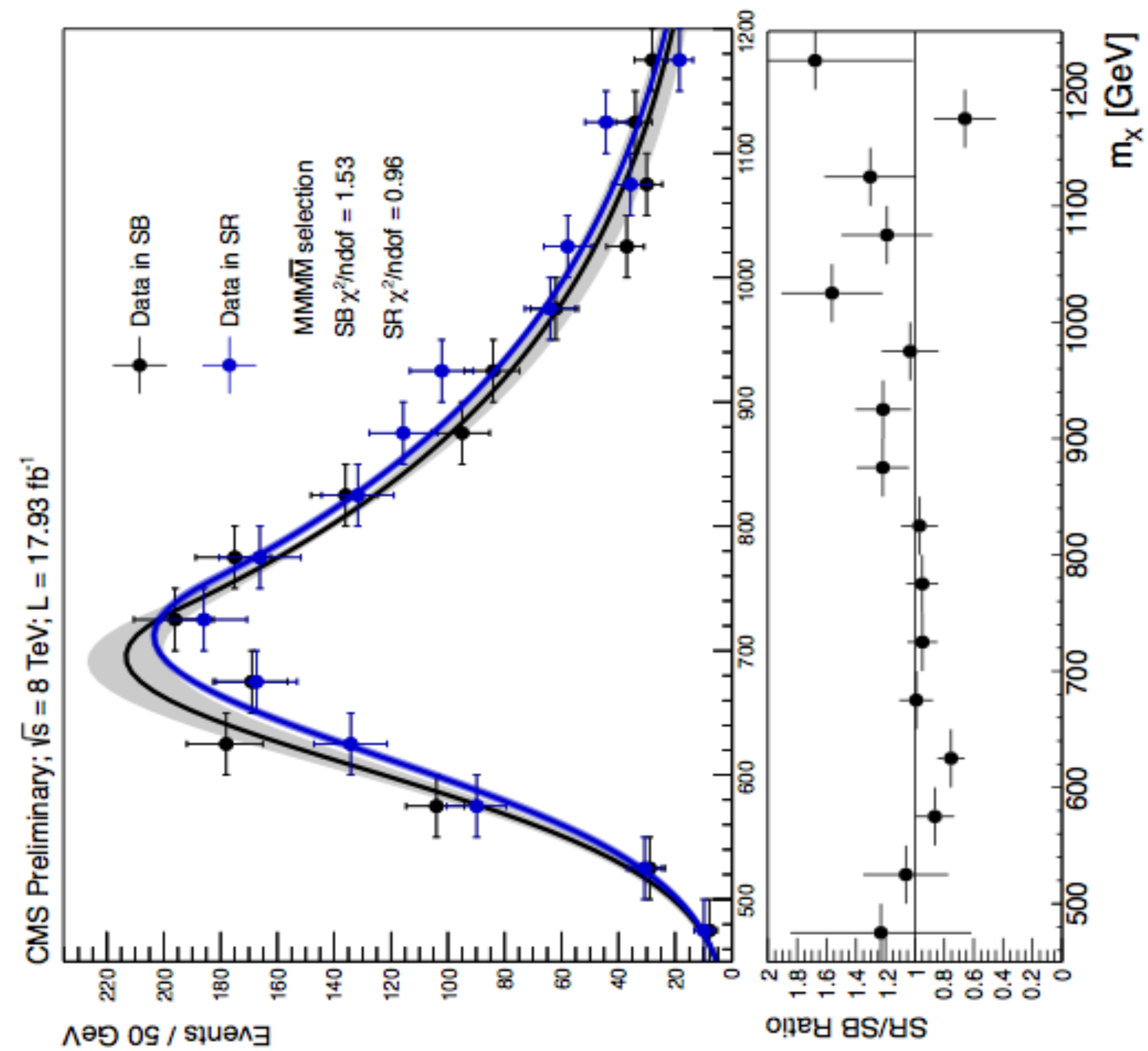

High Mass Region, anti-btag Control Region: The m_X distributions of the QCD multi-jet component of the background in the Validation Region & Sideband (VR & VB) on the left and the Signal Region Sideband (SB) of LMR. The distributions are fitted to the GaussExp function.

$H(b\bar{b})H(b\bar{b})$: Unblinded Data

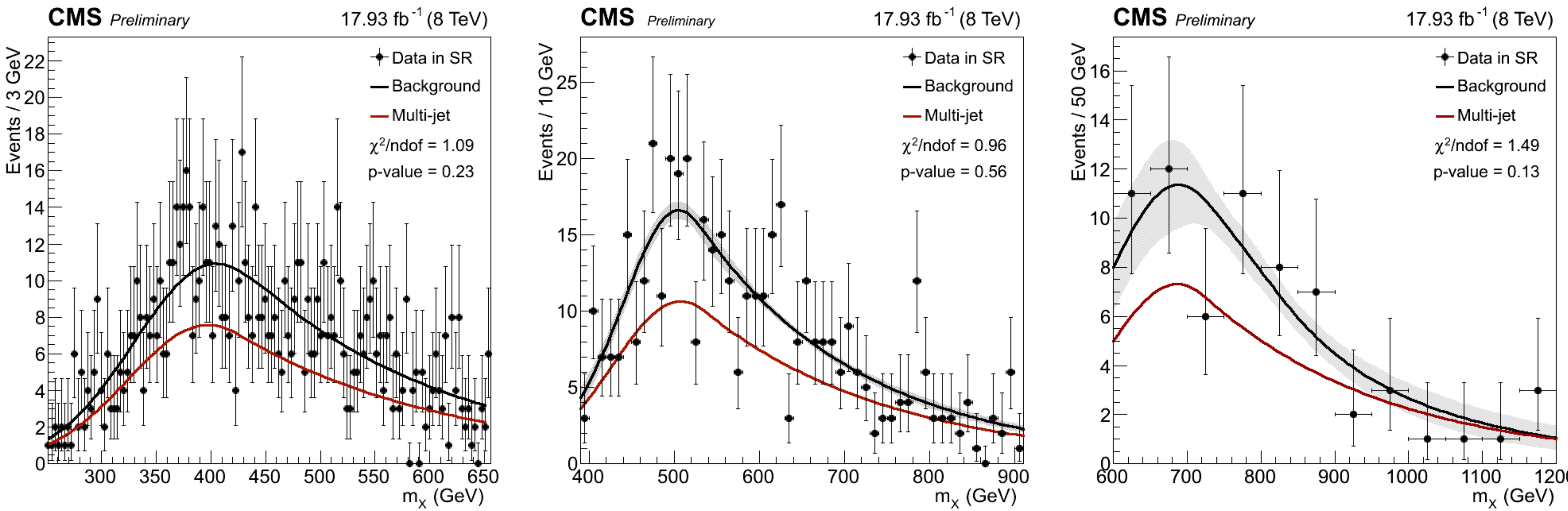

- Background-only fit shown to data in LMR, MMR and HMR. Red curve is the QCD multi-jet contribution. Black curve is QCD multi-jet + tt background.

- Shaded region corresponds to 1σ variation of parameterized fit. Number of degrees of freedom corresponds to the number of fit parameters subtracted from the number of bins in histogram

No clear deviation from background-only hypothesis. Compute upper limits.

$H(b\bar{b})H(b\bar{b})$: Radion Exclusion

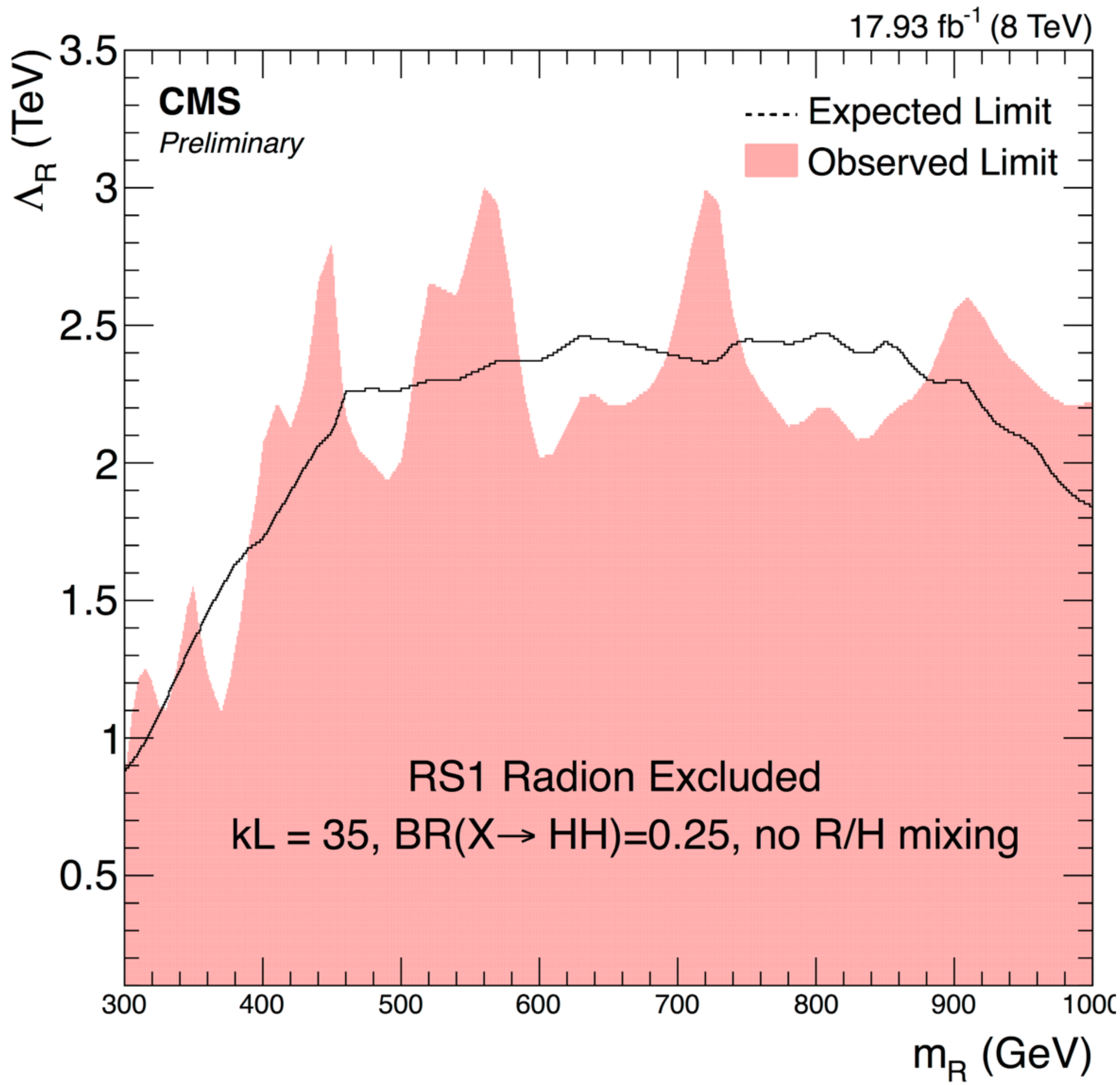

Cross sections of the radion assume *k*-factor for top-loop in gluon-fusion production of R to be identical to that of Higgs production. Also, $Br(R \rightarrow HH) = 0.25$

H($b\bar{b}$)H($b\bar{b}$): Graviton Exclusion

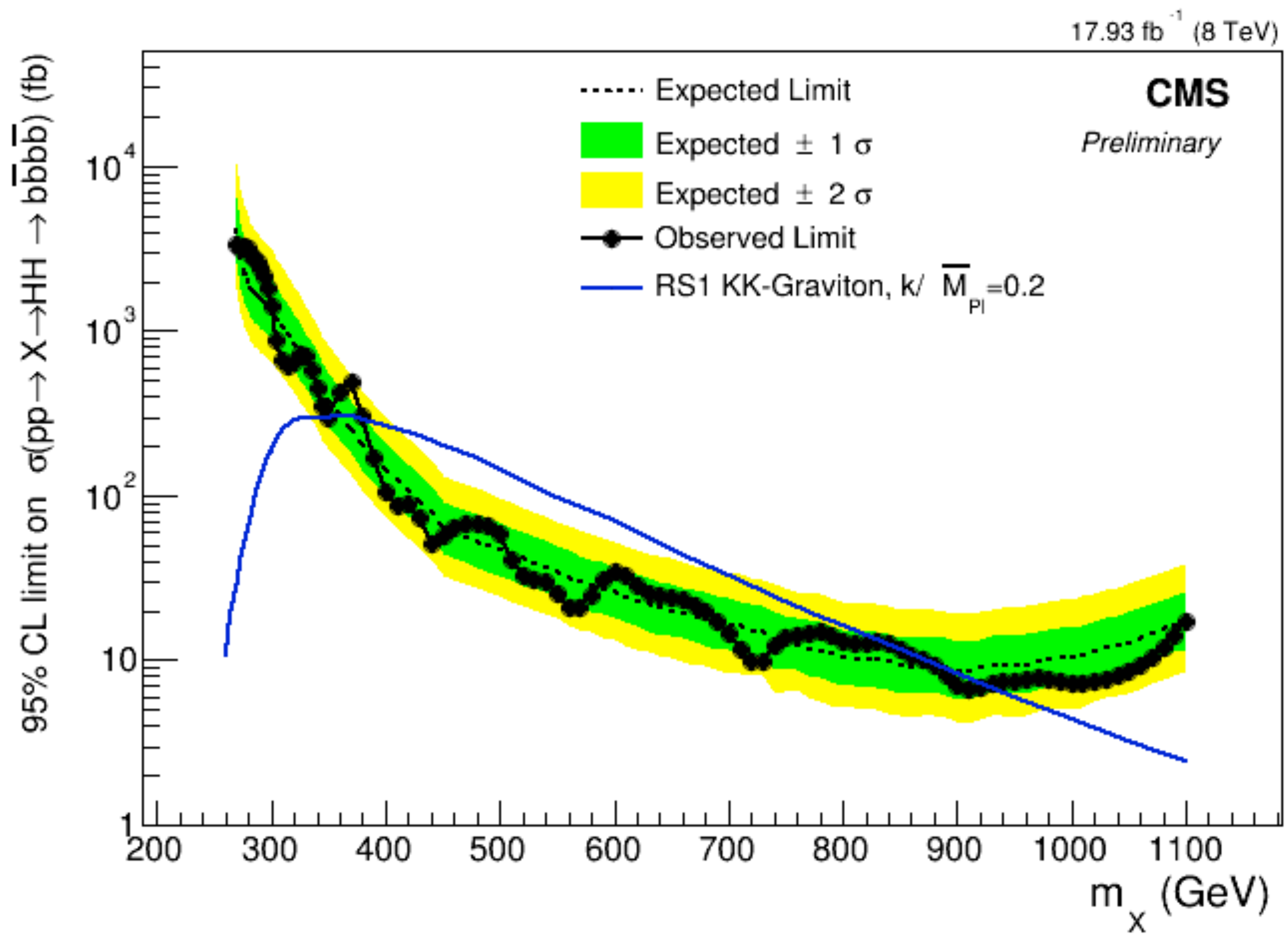

The results are interpreted as upper limit on the production cross section for a spin-2 particle. Signal efficiency is larger than for the spin-0 hypothesis. This results in the exclusion of a smaller cross section. The observed and expected upper limits on the cross section for a spin-2 X to H(bb)H(bb) at 95% confidence level using data corresponding to an integrated luminosity of 17.93/fb at sqrt{s} = 8 TeV using the asymptotic CLs method are shown. Theoretical cross sections for the RS1 KK-Graviton decaying to four b-jets via Higgs bosons are overlaid.

WED scenario: kL = 35, k/M_{Pl}=0.2

CMS double-Higgs: Graviton Exclusion

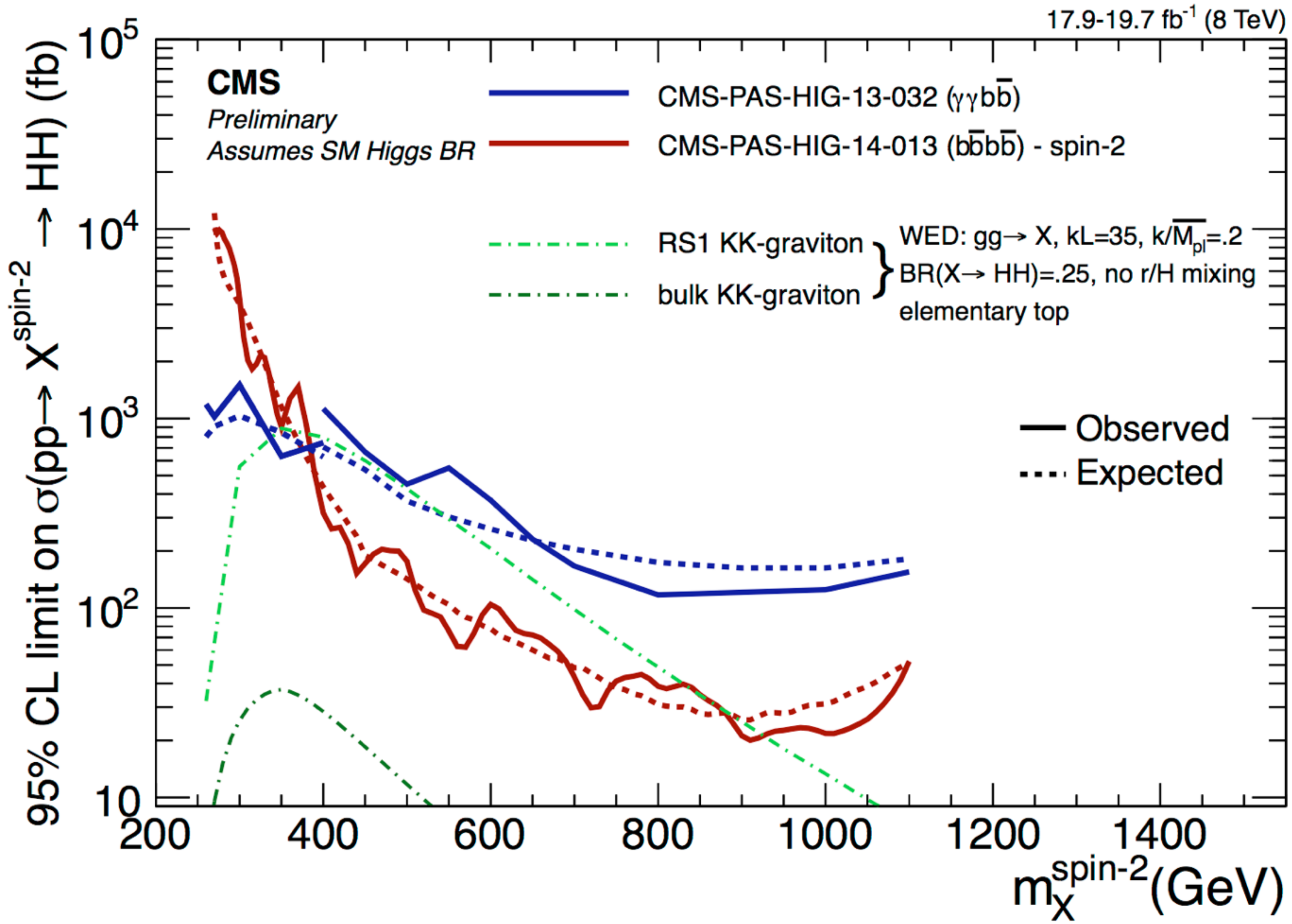

The expected and observed upper limit of spin-2 X to HH production at 95% CLs provided by combining the searches performed by the CMS experiment looking at the $b\bar{b}b\bar{b}$ (HIG-14-013), $b\bar{b}gg$ (HIG-13-032) final states.

WED scenario: kL = 35, k/M_{Pl}=0.2